AD_____

Award Number: DAMD17-98-1-8620

TITLE: Bioenergetic Defects and Oxidative Damage in Transgenic Mouse Models of Neurodegenerative Disorders

PRINCIPAL INVESTIGATOR: Susan E. Browne, Ph.D.

CONTRACTING ORGANIZATION: Weill Medical College of Cornell University
New York, New York 10021

REPORT DATE: May 2002

TYPE OF REPORT: Annual

PREPARED FOR: U.S. Army Medical Research and Materiel Command
Fort Detrick, Maryland 21702-5012

REPORT DOCUMENTATION PAGE

Form Approved
OMB No. 074-0188

1. AGENCY USE ONLY (Leave blank)	2. REPORT DATE	3. REPORT TYPE AND DATES COVERED
	May 2002	Annual (1 May 01 - 30 Apr 02)

4. TITLE AND SUBTITLE
Bioenergetic Defects and Oxidative Damage in Transgenic Mouse Models of Neurodegenerative Disorders

5. FUNDING NUMBERS
DAMD17-98-1-8620

6. AUTHOR(S)
Susan E. Browne, Ph.D.

7. PERFORMING ORGANIZATION NAME(S) AND ADDRESS(ES)
Weill Medical College of Cornell University
New York, New York 10021

sub2001@med.cornell.edu

8. PERFORMING ORGANIZATION REPORT NUMBER

9. SPONSORING / MONITORING AGENCY NAME(S) AND ADDRESS(ES)
U.S. Army Medical Research and Materiel Command
Fort Detrick, Maryland 21702-5012

10. SPONSORING / MONITORING AGENCY REPORT NUMBER

11. SUPPLEMENTARY NOTES
report contains color

12a. DISTRIBUTION / AVAILABILITY STATEMENT
Approved for Public Release; Distribution Unlimited

12b. DISTRIBUTION CODE

13. ABSTRACT ***(Maximum 200 Words)***

This project aimed to determine the contributions of bioenergetic dysfunction and oxidative stress to neurodegeneration in Huntington's disease (HD) and amyotrophic lateral sclerosis (ALS). We found elevations in cerebral glucose utilization in *two* distinctly different mutant mouse models of HD: Hdh^{Q92} and N171-82Q. Hypermetabolism preceded pathologic changes and symptoms, but was not accompanied by alterations in oxidative phosphorylation enzyme activities. We also found late increases in oxidative damage to DNA and lipids in R6/2 and N171-82Q HD mice. Another approach to model HD is to inhibit mitochondrial complex II using the neurotoxin 3-nitropropionic acid (3-NP). In contrast to genetic models, reductions in glucose use following 3-NP coincided with neuronal loss, suggesting a different sequence of pathologic events in this model. In a model of ALS, G93A mice, we also found early metabolic changes preceding neuronal pathology and symptom onset. Reduced glucose utilization in brain and spinal cord at 60 days of age was concomitant with increased mitochondrial complex I activity and depletions in ATP levels. Elevated free radical generation was evident by 90 days. Results clearly demonstrate the early involvement of metabolic changes in the pathologic events initiated by expression of the mutant disease gene in ALS and HD models.

14. SUBJECT TERMS	15. NUMBER OF PAGES
neurotoxin	47
	16. PRICE CODE

17. SECURITY CLASSIFICATION OF REPORT	18. SECURITY CLASSIFICATION OF THIS PAGE	19. SECURITY CLASSIFICATION OF ABSTRACT	20. LIMITATION OF ABSTRACT
Unclassified	Unclassified	Unclassified	Unlimited

FOREWORD

Opinions, interpretations, conclusions and recommendations are those of the author and are not necessarily endorsed by the U.S. Army.

_____ Where copyrighted material is quoted, permission has been obtained to use such material.

_____ Where material from documents designated for limited distribution is quoted, permission has been obtained to use the material.

_____ Citations of commercial organizations and trade names in this report do not constitute an official Department of Army endorsement or approval of the products or services of these organizations.

S.E.B.✓ In conducting research using animals, the investigator(s) adhered to the "Guide for the Care and Use of Laboratory Animals," prepared by the Committee on Care and use of Laboratory Animals of the Institute of Laboratory Resources, national Research Council (NIH Publication No. 86-23, Revised 1985).

_____ For the protection of human subjects, the investigator(s) adhered to policies of applicable Federal Law 45 CFR 46.

_____ In conducting research utilizing recombinant DNA technology, the investigator(s) adhered to current guidelines promulgated by the National Institutes of Health.

_____ In the conduct of research utilizing recombinant DNA, the investigator(s) adhered to the NIH Guidelines for Research Involving Recombinant DNA Molecules.

_____ In the conduct of research involving hazardous organisms, the investigator(s) adhered to the CDC-NIH Guide for Biosafety in Microbiological and Biomedical Laboratories.

Susan Moore 7.30.02.

PI - Signature Date

Table of Contents

5. INTRODUCTION

The goal of this project was to gain insight into the roles of mitochondrial energy metabolism and oxidative stress in the etiology of neuronal degeneration in Huntington's disease (HD) and amyotrophic lateral sclerosis (ALS). The experiments described in the original proposal aimed to determine the relative contributions and sequential order of bioenergetic dysfunction and oxidative damage to the process of cell death in two different transgenic (Tg) mouse models of HD (*Hdh* knock-in mice; R6/2 mice) and one Tg mouse model of familial ALS (G93A SOD1 over-expressors) (White et al, 1997; Mangiarini et al., 1996; Gurney et al., 1994). Over the course of the project, we determined that one of these mouse lines (R6/2 HD mice) develop a diabetic profile that interferes with *in vivo* measurement of cerebral glucose use (Ferrante et al., 2000). Hence, another transgenic mouse line that also expresses a fragment of mutant human huntingtin (N171-82Q mice; Schilling et al., 1999), was substituted for R6/2 mice in some of the experiments. N171-82Q mice develop a phenotype similar to R6/2 mice, but their lifespan is 1-2 months longer. The development of genetically modified mice expressing mutant human transgenes, or mutations in mouse homologues, and that mimic aspects of the human disease phenotype, provide novel opportunities to assess the temporal progression of pathological changes over the course of disease development in an *in vivo* animal model. In addition, the use of mitochondrial toxins allows us to model in animals the cerebral pathogenic sequelae of cell death induced by naturally occurring agents which are potentially extremely hazardous to humans. In this project we used 3-nitropropionic acid (3-NP), a neurotoxin that produces brain lesions and symptoms in humans resembling those seen in HD.

The studies described in this report utilized both *in vivo* and *in vitro* experimental approaches in mutant mice and in rats, to investigate parameters of cerebral energy metabolism (*in vivo* cerebral glucose use measurement by [^{14}C]-2-deoxyglucose autoradiography; NMR lactate imaging; *in vitro* spectrophotometric oxidative phosphorylation enzyme assays; HPLC detection of metabolites), and to investigate the generation of free radicals and oxidative damage products (HPLC detection; immunohistochemistry). The original Specific Aims for the three years of study were:

Year 1: October 1998 - September 1999

1) a) Measurement of local rates of cerebral glucose use ($lCMR_{glc}$) in *Hdh* knock-in mice expressing CAG repeat lengths found in HD patients (48 CAG repeats, Hdh^{Q50}), relative to $lCMR_{glc}$ in wild type littermates (7 CAG repeats, Hdh^{Q7}).

   b) Assessment of any gene dosage effect: Homozygous vs. heterozygous animals.

2) Measurement of electron transport chain activities in *Hdh* knock-in mice with disease-length and normal-length CAG repeats.

3) Measurement of $lCMR_{glc}$ in the G93A human mutant SOD1 over-expression Tg mouse model of ALS. Analysis of the temporal progression of any glucose use changes by measurement at 50, 90 and 120d of age.
4) Electron transport chain enzyme activities in G93A FALS Tg mice at 60 and 120d of age.

Year 2: August 2000 – July 2001

5) Measurement of the effects of increasing CAG repeat number on $lCMR_{glc}$ in *Hdh* knock-in mice (i.e. 90 vs. 48 CAG repeat length).
6) Measurement of $lCMR_{glc}$ in the R6/2 mouse model of HD. Analysis of the temporal progression of any glucose use changes by measurement at 42d, 56d and 84d of age.
7) Measurement of electron transport chain enzyme activities in R6/2 HD mice.
8) NMR assessment of cerebral lactate levels in *Hdh* and R6/2 mice.

Year 3: August 2001 – July 2002

9) Measurement of cerebral levels of oxidative damage markers (protein carbonyls; nDNA OH^8dG; hydroxyl radical production; nitrotyrosine levels) in *Hdh* knock-in and R6/2 HD Tg mouse models.
10) Measurements of oxidative damage markers in G93A FALS Tg mice.
11) HPLC measurement of cerebral energy metabolite levels in HD *Hdh* and R6/2 Tg mice.
12) Measurement of $lCMR_{glc}$ in a rat model of 3-nitropropionic acid neurotoxicity.

NB: during the course of this grant, PI Dr. Susan Browne and Co-PI Dr. M. Flint Beal moved laboratories from Massachussetts General Hospital, Boston, MA, to Weill Medical College of Cornell University in New York, NY. This resulted in a delay in funding during grant transferal (September 1999 to August 2000). There was also some delay while mutant mouse colonies were re-established in the New York laboratory, which required a concerted effort at the start of the second year.

6. BODY

The pathogenetic mechanisms in both Huntington's disease (HD) and amyotrophic lateral sclerosis (ALS) are still unclear, however, in both cases *in vivo* and *in vitro* studies implicate the involvement of bioenergetic defects in the disease process (for review, see Browne and Beal, 2000; Menzies et al., 2002). Attempts to ascertain the role of energetic dysfunction in pathogenesis have been greatly enhanced by the development of several different transgenic mouse lines replicating aspects of each disorder. HD models express the huntingtin gene mutation underlying HD, an abnormal expansion of the polyglutamine (Q) domain in huntingtin protein, encoded by an expanded triplet (CAG) repeat in exon 1 of the huntingtin gene. Familial ALS (FALS) models express some of the multiple Cu/Zn superoxide dismutase (SOD1) mutations that occur in approximately 25% of familial ALS patients. These models allow novel determinations of metabolic parameters over the life-span of the animals, before, during and after onset of pathological changes and disease symptoms. HD mouse lines differ in terms of the site of mutant gene incorporation, CAG repeat length, copy number, and promoter used, and these differences are reflected in the phenotypes of the mice generated. Studies in this project utilize *Hdh* CAG knock-in mice (White et al., 1997), R6/2 transgenic mice overexpressing an N-terminal fragment of human mutant huntingtin, including a 145 polyglutamine repeat stretch (Mangiarini et al., 1996), and N171-82Q mice also expressing an N-terminal fragment of human mutant huntingtin, but with a shorter (82Q) polyglutamine repeat stretch (Schilling et al., 1999). The ALS mouse model employed is the G93A model (Gurney et al., 1994), overexpressing a human SOD1 glycine to alanine mutation. In the thrid year of this project we also utilized a neurotoxin model of HD, using 3-nitropropionic acid (3-NP) to induce striatal-specific brain lesions with a concomitant movement disorder in rats. Model characteristics are discussed in detail in the relevant section below. Summaries of the outcomes of each of the research objectives of this project follow, in chronological order of the annual Aims.

YEAR 1

Objective #1: **To investigate the effect of expressing 48 CAG repeats – a CAG repeat length consistent with the generation of mutant huntingtin HD patients – on local rates of cerebral glucose use (lCMRglc) in the Hdh mouse model of HD; and to assess any gene dosage effect.**

Hdh CAG "knock-in" mice were developed by inserting CAG repeats into exon 1 of the murine huntingtin homologue (*Hdh)* to generate a set of precise genetic HD mouse models which accurately express mutant huntingtin protein (White et al., 1997). Mice expressing 50 or 92 glutamines (encoded by the CAG repeat domains), Hdh^{Q50} and Hdh^{Q92} respectively, do not develop any overt behavioral phenotype over their lifespan. However, they do show cellular changes

involving translocation of mutant huntingtin from the cytosol to the nucleus, and formation of intranuclear aggregates or inclusions (NII) containing ubiquitinated mutant huntingtin. The time at which these events occur is CAG repeat length-dependent, occurring earlier in Hdh^{Q92} mice (nuclear huntingin is evident by ~4 months of age; aggregates form by 15 months; Wheeler et al., 2000). Hdh^{Q111} mice expressing a longer polyglutamine stretch have recently been reported (Wheeler et al., 2002). These mice show expedited aggregate formation (by about 6 months of age), and also display a mild behavioral phenotype and striatal-specific cell degeneration by approximately 19 months of age. All mice have normal life-spans.

In this study we used [^{14}C]-2-deoxyglucose *in vivo* autoradiography in four month-old $\boldsymbol{Hdh^{Q50}}$ knock-in mice (time-point chosen to precede pathological changes), expressing a CAG repeat that causes HD in humans (48 CAGs), to determine:

- if cerebral glucose utilization is altered by this HD mutation, and
- the effect of gene dosage on glucose use (homozygous versus heterozygote mice).

We used a modification of the [^{14}C]-2-deoxyglucose *in vivo* autoradiography technique developed by Sokoloff and colleagues (Sokoloff 1977) to measure local rates of cerebral glucose use ($lCMR_{glc}$) in *Hdh* "knock-in" mice (Browne et al., 1999). The [^{14}C]-2-deoxyglucose (2-DG) procedure facilitates localization and quantitation of $lCMR_{glc}$ in discrete anatomical regions throughout the CNS of conscious animals. It's utility is based on the premise that glucose is the primary energy source for cerebral cells, but brain tissue has a minimal capacity to store carbohydrates and therefore relies on glucose extraction from the circulation to fulfill energy demands. Thus, changes in glucose use generally reflect alterations in functional activity within CNS regions. Regional measurement of the rate of uptake of a radiolabelled glucose analog, ^{14}C-2-deoxyglucose, from the blood allows *in vivo* estimation of local rates of energy metabolism. Briefly, the procedure involves surgical implantation of femoral arterial and venous catheters; i.v. administration of [^{14}C]-2-deoxyglucose to the conscious mice; repeated arterial blood sampling for ^{14}C and plasma glucose measures; blood gas analysis; decapitation and brain harvest; cryostat processing of brain into 20μm-thick coronal sections throughout brain; exposure to film with pre-calibrated standards; densitometric measurement of regional ^{14}C levels from autoradiograms and estimation of regional glucose utilization rates.

Animals: Experiments employed 18 mice in three groups: *Hdh* mice both homozygous and heterozygous for the transgene, expressing 50 (Hdh^{Q50}) glutamines (48/48 and 48/7 CAG repeats, respectively) and in normal wild-type littermates (Hdh^{Q7}, 7/7 CAGs). Three mice were excluded from the 2-DG procedure analysis due to abnormal glucose or blood gas levels, indicating non-physiologically normal mice, and one mouse died during surgery.

Physiological variables: Arterial plasma glucose concentration, *p*O2, *p*CO2 and *p*H were measured 35 minutes into the procedure (10 minutes before animal decapitation) to determine the physiological status of the animals (Table 1). There were no significant differences in the levels of any of these measured parameters between 7/7, 48/7 and 48/48 mice ($p > 0.05$, ANOVA, followed by Fisher's PLSD). All measured parameters were within accepted normal ranges, indicating that there are no physiological effects associated with the *Hdh* mutation which might impact on the interpretation of glucose use results. In separate studies we have assessed glucose tolerance in *Hdh* mutant mice, in light of reports that R6/2 mice develop diabetes. We found that neither *Hdh* Q7, Q50, Q92 or Q111 showed any evidence of hyperglycemia or abnormal glucose handling (data not shown).

Table 1: Physiological variables in *Hdh* ^{Q50} CAG Knock-in Mice

Variable	7/7	48/7	48/48
Arterial Glucose (mg/dL)	133.2 ± 6.0	154.3 ± 10.1	134.8 ± 6.6
pO_2 (mmHg)	92.6 ± 2.4	91.8 ± 4.2	85.5 ± 2.7
pCO_2 (mmHg)	39.7 ± 1.8	40.3 ± 1.7	39.6 ± 1.2
*p*H	7.4 ± 0.0	7.4 ± 0.0	7.4 ± 0.0

Data are mean ± SEM, variables measured 35 min after initiation of the [^{14}C]-2-deoxyglucose procedure in *Hdh*^{Q7} (7/7) and *Hdh*^{Q50} (48/7 and 48/48) knock-in mice (n=4-6 per group). There were no statistically significant differences between 48/7, 48/48 and 7/7 mice in any of the parameters measured ($p>0.05$, ANOVA).

Local Cerebral Glucose Use, lCMR$_{glc}$: We measured cerebral metabolic rates for glucose in 21 brain regions. Glucose use values in each of the brain regions examined are presented in Table 2. Glucose use rates did not significantly differ between *Hdh*^{Q50} and *Hdh*^{Q7} mice in any of the brain regions examined ($p > 0.05$; ANOVA, followed by Fisher's PLSD), and there was no effect of gene dosage in *Hdh*^{Q50} mice (48/48 vs 48/7).

Discussion: Results suggest that cerebral glucose use rates do not differ between *Hdh*^{Q50} and *Hdh*^{Q7} mice in any of the brain regions examined in four month-old mice. Consequently, there was also no observable gene dosage effect in *Hdh*^{Q50} mice (48/48 vs 48/7). This contrasts with the pilot results presented in the original grant proposal, which suggested that glucose use showed a slight elevation in 48/48 mice relative to levels in wild type (7/7, 7/0) mice. This difference in outcome most likely reflects increased variance associated with larger group sizes for investigation. Observations by Wheeler et al. (2000) suggest that both translocation of huntingtin protein from cytosol to the nucleus, and NII formation, are CAG repeat length-dependent processes. Therefore, there is reason to suppose that energetic changes in *Hdh* mice may also vary in time of onset depending on CAG repeat length. Subsequently, studies were extended to mice expressing longer CAG repeats (*Hdh*^{Q92}) in Year 2 of this project (see "Objective # 5").

Table 2: Local Cerebral Glucose Utilization ($lCMR_{glc}$) in *Hdh* ^{Q50} CAG Knock-in Mice

Region	7/7	48/7	48/48
Frontal Cortex	43.3 ± 2.8	45.7 ± 3.3	41.3 ± 4.7
Parietal Cortex	41.3 ± 2.5	43.8 ± 4.1	40.8 ± 4.0
Anterior Cingulate Cortex	55.0 ± 2.0	61.5 ± 6.1	56.9 ± 6.7
Auditory Cortex	50.3 ± 6.2	49.9 ± 3.8	48.7 ± 4.2
Striatum: Dorsolateral	47.5 ± 5.4	51.7 ± 5.3	46.1 ± 4.2
Ventromedial	46.0 ± 5.2	48.4 ± 4.6	45.3 ± 4.7
Globus Pallidus	29.2 ± 2.1	28.7 ± 2.5	29.2 ± 2.1
Hippocampus: CA1	27.8 ± 2.2	28.8 ± 2.6	25.7 ± 2.9
CA3	34.9 ± 2.2	37.7 ± 3.0	33.8 ± 3.9
Dentate Gyrus: Molecular Layer	45.2 ± 3.5	40.2 ± 2.8	41.7 ± 4.0
Dorsolateral Geniculate Body	42.6 ± 3.1	44.3 ± 2.9	42.7 ± 6.4
Medial Geniculate Body	46.1 ± 3.7	57.7 ± 5.3	48.7 ± 7.0
Superior Colliculus: Superficial Layer	38.2 ± 2.9	37.8 ± 2.9	36.2 ± 4.5
Deep Layer	38.5 ± 2.0	37.1 ± 2.6	37.1 ± 4.8
Internal Capsule	14.4 ± 2.0	15.5 ± 2.5	12.4 ± 2.2
Thalamus: Dorsomedial	46.1 ± 2.9	45.4 ± 4.8	44.8 ± 5.4
Ventromedial	34.9 ± 2.2	37.7 ± 3.0	33.8 ± 3.9
Substantia Nigra: *pars reticulata*	24.7 ± 1.8	27.9 ± 2.3	25.0 ± 3.6
pars compacta	44.6 ± 3.5	43.9 ± 3.1	40.1 ± 5.4
Cerebellum: Grey matter	28.4 ± 1.5	29.7 ± 2.6	26.8 ± 3.2
White matter	18.6 ± 1.6	19.8 ± 3.1	17.3 ± 2.0

Local cerebral metabolic rates for glucose (nmol/100g/min) in homozygous (48/48) and heterozygous (48/7) *Hdh*^{Q50} knock-in mice, compared with rates in wild-type (7/7; *Hdh*^{Q7}) littermate controls (n=4-6 per group).
Data presented as mean ± SEM. There were no statistically significant differences between glucose use in 48/48 and 48/7 *Hdh*^{Q50} mice and littermate wild-type controls ($p > 0.05$, ANOVA).

Objective #2: **Measurement of electron transport chain activities in *Hdh* knock-in mice with disease-length and normal-length CAG repeats.**

We used spectrophotometric assays to measure the activities of the mitochondrial electron transport chain enzyme complexes I, II-III and IV, in homogenate preparations of *Hdh* mouse cerebral forebrain and cerebellum (according to the methods outlined in the proposal). We also extended spectrophotometric studies from the original SOW, to measure activity of the tri-carboxylic acid (TCA) cycle enzyme aconitase in the same animal population. Aconitase is of particular interest as its' activity has been shown to be markedly reduced in post-mortem tissue from late stage HD patients (Tabrizi et al., 1999), and the same group have also reported reduced levels of activity in HD skeletal muscle (Lodi et al., 2000). Enzyme activities per mg protein were corrected by citrate synthase activity per mg protein, to account for the possibility of neuronal or mitochondrial loss.

Animals: Enzyme activities were measured in 4 month old Hdh^{Q7} (7/7 CAG repeats), Hdh^{Q50} (48/7 and 48/48 CAG repeats), and Hdh^{Q92} (90/7 and 90/90 CAG repeats). This time-point was chosen to precede any pathologic changes in these mice, and to correlate with glucose utilization studies conducted in same age mice.

Enzyme Activities: Results in 4 month-old mice are shown in Figures 1 and 2. There were no significant alterations in citrate synthase activities in any of the mouse genotypes examined, in forebrain or cerebellum (Figure 1). This indicates no significant loss of neurons and/or mitochondria at this time point. Complex activities were unaltered in Hdh^{Q92} *and* Hdh^{Q50} mice in forebrain homogenates ($p > 0.05$; ANOVA, followed by Fisher's PLSD), although there was evidence of a trend towards reduced complex II-III and IV activities with increasing CAG repeat number (see Figure 2). In cerebellum homogenates, however, complex II-III was reduced in 48/7 mice (-38%, $p<0.05$) and showed a trend to decrease in 90/7 and 90/90 mice (-36% and –24%, respectively). Complex IV activity was also significantly reduced in 48/7 and 90/90 mouse cerebellum (-35% and -42%, respectively; $p<0.01$), whilst trends towards reduced activity are evident in 48/48 and 90/90 mice (-18 and –31%, respectively).

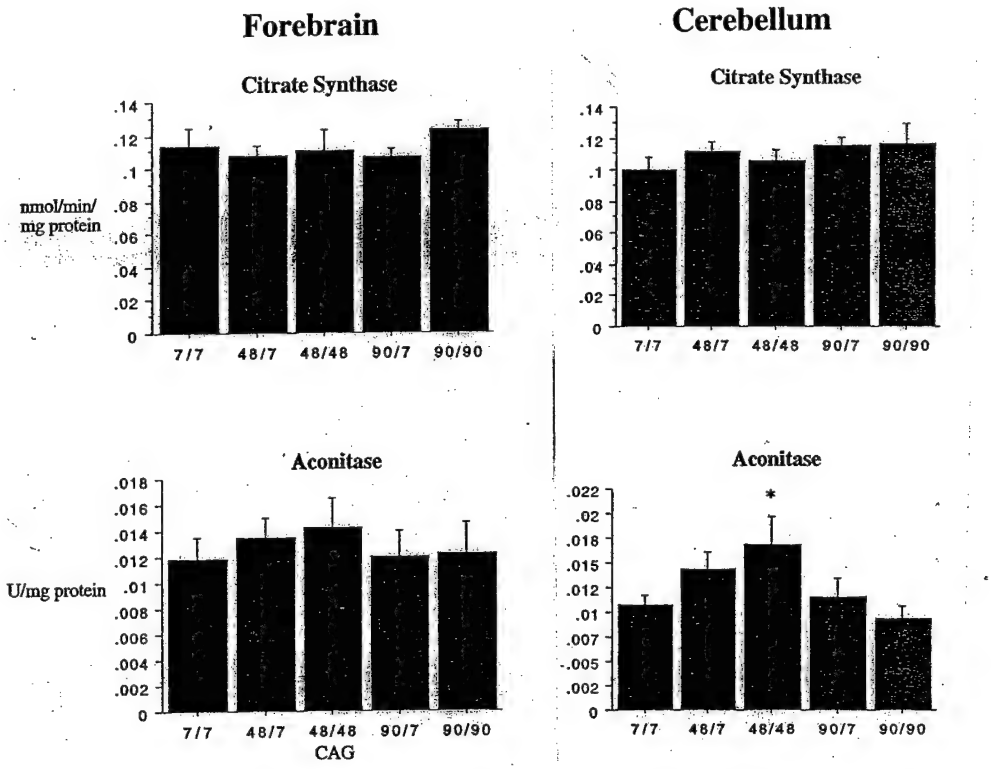

Figure 1: TCA Cycle Enzyme Activities in Hdh^{Q7}, Hdh^{Q50}, and Hdh^{Q92} Brains: 4 Months
Data are presented as mean ± SEM citrate synthase (CS) activity (nmol/min/mg protein) and aconitase activity (U activity/mg protein) in forebrain and cerebellum homogenates. Subjects were 4 month-old CAG knock-in mice, expressing wild type (7/7) or mutant (48/7, 48/48, 90/7, 90/90) length CAG repeats in huntingtin protein.
* $p <$ 0.05, significant difference relative to wild type control mice (ANOVA, and post-hoc Fisher PLSD).

Complex I activity in cerebellum also showed a small, significant reduction in activity in 48/7 mice, relative to levels in wild type mice (-19%; $p<0.05$), but was unaltered in other genotypes. Aconitase activity was unaltered in forebrain, but showed an increase in 48/48 mice in cerebellum, although 90/7 and 90/90 levels did not differ from wildtype levels (Figure 1). The reason for this alteration is currently unclear.

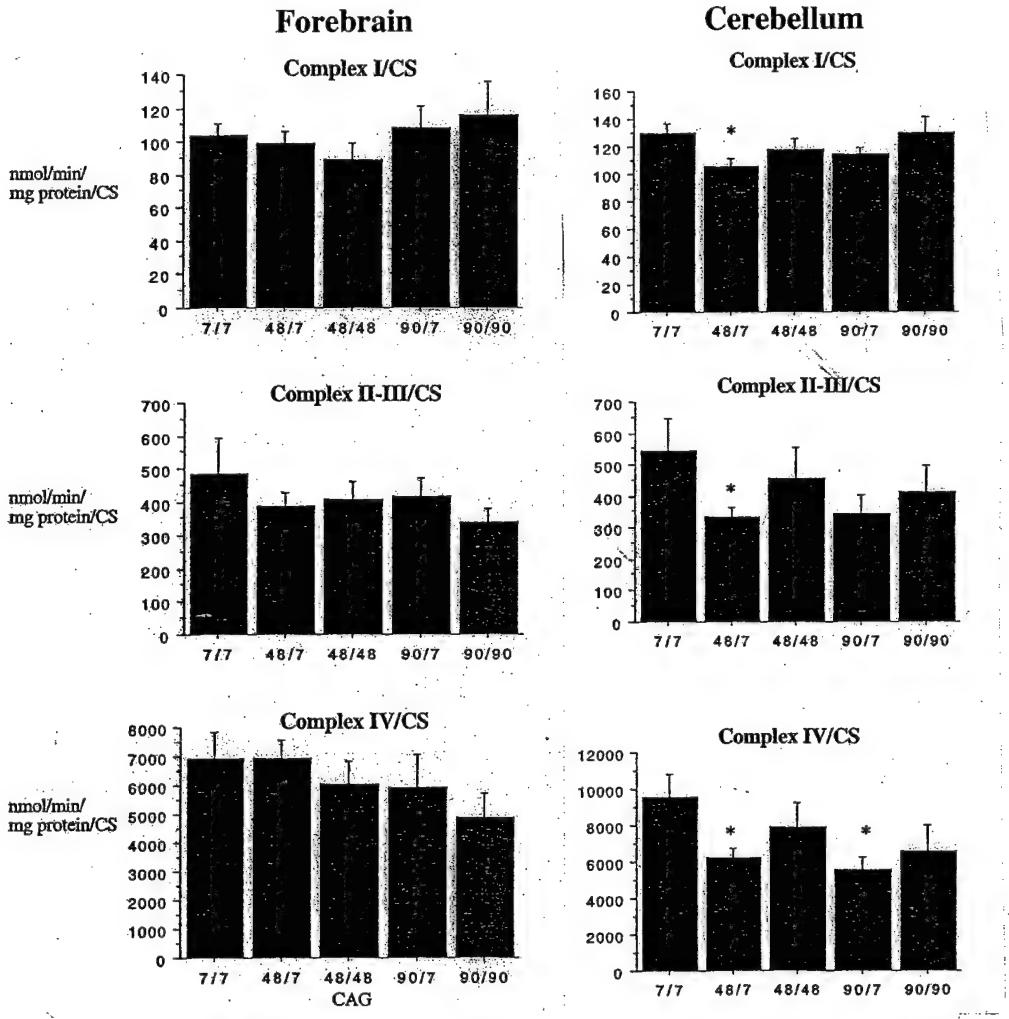

Figure 2: Mitochondrial Respiratory Enzyme Activities in Hdh^{Q7}, Hdh^{Q50}, and Hdh^{Q92} Brains: 4 months
Data are presented as mean ± SEM citrate synthase (CS)-corrected complex activities (nmol/min/mg protein/CS) in forebrain and cerebellum homogenates. Subjects were 4 month-old CAG knock-in mice, expressing wild type (7/7) or mutant (48/7, 48/48, 90/7, 90/90) length CAG repeats in huntingtin protein.
* $p < 0.05$, significant difference relative to wild type control mice (ANOVA, and post-hoc Fisher PLSD).

Discussion: These results suggest that there is some degree of impairment of complex II-III and IV activities in Hdh^{Q92} *and* Hdh^{Q50} mice, reaching statistical significance in the cerebellum. It is possible that region-specific changes occurring in forebrain structures may be being masked by measuring enzyme activities in the whole forebrain.

Objective #3: **Measurement of $lCMR_{glc}$ in the G93A human mutant SOD1 overexpression Tg mouse model of ALS. Analysis of the temporal progression of any glucose use changes by measurement at 60, 90 and 120d of age.**

Transgenic mice overexpressing a human mutant form of SOD1 (a glycine to alanine substitution in exon 4, G93A) develop a disease syndrome whose neuropathology and neurological symptoms closely resemble human ALS (Gurney et al, 1994; Dal Canto and Gurney, 1995). Animals show signs of hind limb weakness at approximately 90-110 days of age, and gradually become paralyzed before dying at 150-180d. Numerous Lewy Body-like inclusions are seen at late stages of the disease. Neuropathological changes including microvesiculation are evident prior to the development of neurological symptoms (≈70 days). The involvement of mitochondrial energy metabolism dysfunction in the pathogenesis of this motor disorder is supported by observations that the first pathological events identified in these mice are membrane blebbing and vesiculation of the mitochondria (Dal Canto and Gurney, 1995). The hypothesis of a gain of function mutant SOD1 is supported by findings that animals expressing high levels of human wild type SOD do not develop the clinical disease, and a recent report that transgene expression levels correspond with the degree of neurotoxicity in mice. The aim of our study was to determine whether there is evidence in this mouse model of FALS of any alterations in energy metabolism prior to the onset of symptoms and mitochondrial morphological changes. We also endeavored to determine the pattern of glucose use changes over the lifespan of these animals.

Animals: Experiments employed 46 G93A and wildtype littermate mice, at 60, 90 and 120 days of age. Fourteen mice were excluded prior to the 2-DG procedure, due to death during surgery (n=4), poor blood flow in the femoral catheters (n=7), or abnormally high pre-glucose levels (n=3). Thirty-two mice underwent the 2-DG procedure at 60 days of age (n=9), 90 days (n=12), and 120 days (n=11). Of these, several were excluded from the final glucose use analysis due to poor blood gases, death during the procedure (due to mice pulling out their arterial catheters), abnormal arterial glucose levels, or poor radionuclide perfusion. Final group sizes after analysis were 2-9 per group. We encountered many difficulties in achieving optimal physiological conditions and isotope delivery in this strain of mice. Consequently, we have not included 90 day glucose use values in the results below as the group sizes were too small to analyze statistically. Experiments have been repeated in an additional 21 mice to date in the third year of this project. We also extended studies to 120 day-old N1029 mice that overexpress a transgene of human non-mutant SOD-1 (n = 15). N1029 mice will serve as a transgenic control for the G93A mice. Glucose use values from these latter studies are still being analyzed densitometrically. Data are presented for the original study.

Physiological Variables: Multiple physiological parameters in G93A and wild-type were assessed during the 2-DG experimental period, to determine whether any experimental group displayed

physiologic changes which might impact on glucose utilization (Table 3). All measured parameters were within normal physiological limits for all experimental groups, at all ages. There were no significant differences in any of the measured parameters between G93A and wild-type littermate mice (ANOVA, $p>0.05$). Arterial plasma glucose levels within groups did not significantly alter over the course of the experiments (Student's paired t-test, $p>0.05$), indicating that mice are not abnormally stressed as a direct result of the experimental procedure.

Table 3: Physiological Variables in G93A FALS Mice (Mean ± SEM).

	Wildtype 60d	**G93A** 60d	**Wildtype** 120d	**G93A** 120d
Pre-Glucose (mg/dL)	147 ± 6	167 ± 10	118 ± 7	129 ± 12
Glucose End (mg/dL)	160 ± 12	192 ± 10	119 ± 4	140 ± 10
p_aO_2 (mm Hg)	117 ± 5	112 ± 3	97 ± 2	93 ± 7
p_aCO_2 (mm Hg)	36 ± 1	39 ± 2	28 ± 3	33 ± 3
***p*H**	7.33 ± 0.01	7.33 ± 0.01	7.40 ± 0.03	7.34 ± 0.02
N	8	9	3	5

Rates of Cerebral Glucose Use: Glucose use rates were calculated in multiple brain regions and 9 spinal cord regions in transgenic G93A mice and wildtype littermates at ages preceding pathological changes (60 days), and at end-stage of the disorder (120-123d) (Figure 3). Marked reductions in glucose use were evident in frontal cortex, motor cortex and striatum of G93A SOD1 mice as early as 60 days of age, relative to levels in wild type littermates. This pattern of glucose use reduction was still evident in 120 day-old mice relative to levels in wild-type mice, although non-transgenic wild type glucose use levels were also decreased at this time point, relative to levels at 60 days.

Discussion: This initial study demonstrates a marked reduction in glucose use is evident in frontal cortex, motor cortex and striatum of G93A SOD1 mice at 60 days, relative to levels in wild type littermates. This pattern of glucose use reduction is still evident at 120 days of age, although transgenic wild type glucose use levels are also decreased at this time point, relative to levels at 60 days. These results suggest that glucose metabolism in the forebrain is impaired at 60 days of age in G93A SOD1 mice, and that this impairment precedes mitochondrial pathology in this FALS model. As noted above, further experiments are under analysis to extend these observations.

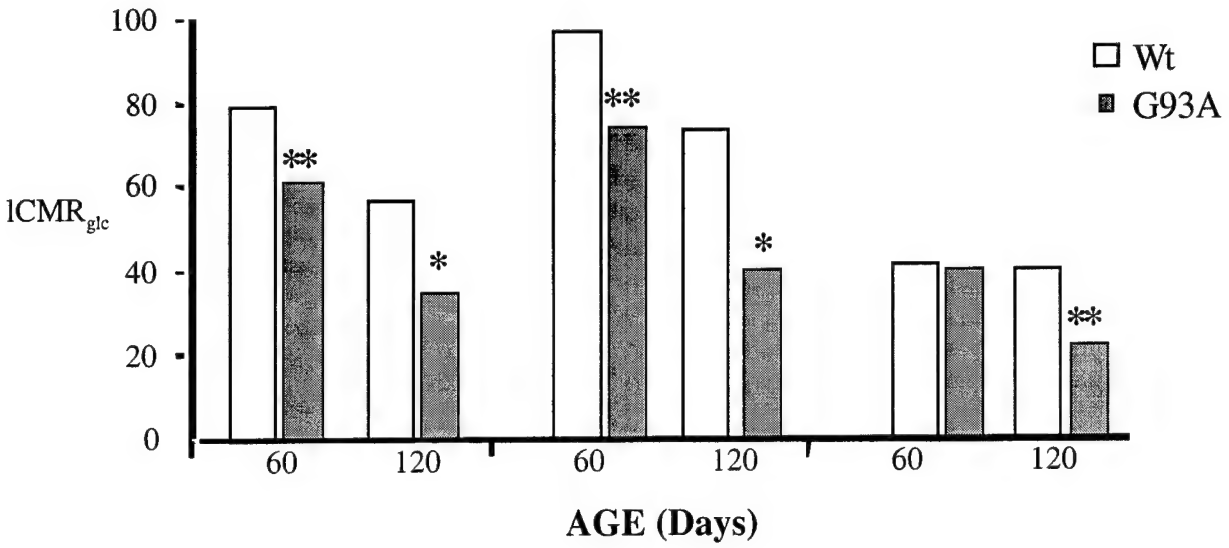

Figure 3: Time Course of Cerebral Glucose Use (lCMR$_{glc}$) Changes in G93A SOD1 Mice

lCMR$_{glc}$ (nmol/100g/min) in G93A SOD1 mutant mice and G93A wild type littermate controls (Wt). Data are mean ± SEM. * $p<0.05$, ** $p<0.01$, significant difference between G93A and age-matched Wt mice (Student's unpaired t-test).

Discussion: This initial study demonstrates a marked reduction in glucose use in frontal cortex, motor cortex and striatum of G93A SOD1 mice at 60 days, relative to levels in wild type littermates. This pattern of glucose use reduction is still evident at 120 days of age, although glucose use levels in wildtype littermate mice are also decreased at this time point, relative to levels at 60 days. These results suggest that glucose metabolism in the forebrain is impaired at 60 days of age in G93A SOD1 mice, and that this impairment precedes mitochondrial pathology in this FALS model. As noted above, further experiments are under analysis to extend these observations.

Objective #4. **Measurement of the temporal profiles of electron transport chain activities in the G93A FALS Tg mouse model of FALS**

We augmented the glucose use studies of energy metabolism by investigating mitochondrial respiratory transport chain activities and SOD1 levels using spectrophotometric assays.

Animals: Metabolic enzyme activities were measured in pre-symptomatic (60 day old) G93A SOD1 mice, in homogenate preparations of whole forebrain, brainstem and spinal cord, and cerebellum. We compared enzyme activities with levels in N1029 transgenic wild type controls (Tg-Wt) and non-transgenic wild type littermate controls (Wt). We also measured electron transport enzyme activities in 100-104 day-old G93A mice. Experiments used 53 mice.

Enzyme Activities: a) Results in 60 day-old mice are presented in Table 4. Complex I activity was significantly increased in G93A SOD1 mouse forebrain, relative to levels in Tg-Wt mice at this time-point. In contrast, in G93A spinal cord/brainstem, complex I activity was decreased compared with

Wt levels (but not Tg-Wt). In addition, complex IV activity was reduced in the spinal cord/brainstem and cerebellum of G93A mice. Both Tg-Wt and G93A SOD1 mice expressed equivalent levels of cytosolic SOD1 activity (9.4 ± 0.3 vs. 11.4 ± 0.4 Units/mg protein, respectively), which were significantly higher than SOD1 levels in non-Tg Wt mice ($p<0.05$). b) We also measured respiratory chain enzyme activities in the forebrain of 100-104 day-old G93A mice (Table 5). The pattern of elevated complex I activity with no changes in complexes II-III and IV , seen in 60 day mice, is conserved in the forebrain at 100 days of age.

Table 4: Metabolic enzyme activities in 60 day-old G93A and control mice

		Forebrain	Spinal Cord/ Brainstem	Cerebellum
Complex I	**Wt**	**145 ± 11**	**111 ± 7**	**88 ± 7**
(nmol/min/mg protein/CS)	**Tg Wt**	**130 ± 7**	**104 ± 6**	**84 ± 5**
	G93A	**162 ± 6 ****	**91 ± 5 †**	**74 ± 7**
Complex II-III	**Wt**	**3.06 ± 0.1**	**1.40 ± 0.1**	**1.66 ± 0.1**
(nmol/min/mg protein/CS)	**Tg Wt**	**3.15 ± 0.3**	**1.38 ± 0.1**	**1.75 ± 0.1**
	G93A	**3.99 ± 0.2**	**1.48 ± 0.1**	**1.54 ± 0.2**
Complex IV	**Wt**	**3.77 ± 0.2**	**1.62 ± 0.1**	**1.81 ± 0.1**
(nmol/min/mg protein/CS)	**Tg Wt**	**3.22 ± 0.3**	**1.40 ± 0.1**	**1.52 ± 0.1 †**
	G93A	**4.41 ± 0.5**	**1.36 ± 0.1 †**	**1.19 ± 0.1*†**
Cu/Zn SOD	**Wt**	**5.3 ± 0.6**		
(U/mg protein)	**Tg Wt**	**9.4 ± 0.3 †**		
	G93A	**11.4 ± 0.4 **†**		

Data are mean ± SEM citrate synthase (CS)-corrected complex activities (nmol/min/mg protein/CS) and Cu/Zn SOD activity (U/mg protein). Activities measured in forebrain, spinal cord/brainstem, and cerebellum of G93A mice, and age-matched N1029 transgenic wildtype mice (TgWt) and littermate wildtype controls (Wt). N = 6-16/group.
* $p<0.05$, ** $p<0.05$ significant increase vs Wt Tg (N1029). † $p<0.05$ Change vs Wt (ANOVA, and post-hoc Fisher PLSD).

Table 5: Mitochondrial Respiratory Enzyme and SOD1 Activities in G93A Transgenic Mice:100-104days

	n	Complex I	Complex II-III	Complex IV	Cu/Zn SOD
Wild Type	7	293 ± 22	1.04 ± 0.04	1.14 ± 0.15	4.2 ± 0.1
Tg-Wild Type	7	354 ± 28	1.08 ± 0.09	1.38 ± 0.14	12.4 ± 0.8
G93A	7	386 ± 6 *	1.18 ± 0.12	1.48 ± 0.19	13.4 ± 0.49

Data presented as mean ± SEM citrate synthase (CS)-corrected complex activities (nmol/min/mg protein/CS) and Cu/Zn SOD activity (U activity/mg protein) in cortical mitochondrial fractions and cytosol, respectively. Subjects were G93A mice Tg-wildtype (N1029), and wild type control mice (age range: 100-104d). * $p < 0.05$, significant difference relative relative to wild type control mice (ANOVA, and post-hoc Fisher PLSD).

Discussion: These findings suggest that the gene defect in G93A mice induces alterations in electron transport chain enzyme activities in forebrain and spinal cord/brainstem regions of the CNS. These alterations are not attributable simply to overexpression of human SOD1, since similar changes do not occur in Tg-Wt (N1029) mice overexpressing normal human SOD1. The observation of elevated complex I activity in G93A SOD1 mice is consistent with our previous findings of increased complex I activity in cortical regions of FALS patients with the A4V SOD1 mutation (Browne et al., 1998). Results support the suggestion arising from cerebral glucose use observations in "Objective #3", that that metabolic defects may exist before signs of motor impairment (about 90 days) and pathological abnormalities (about 70 days). Further evidence supporting this hypothesis comes from recent findings in this laboratory that levels of the energy metabolite ATP are markedly reduced in G93A mice as early as 30 days in forebrain and spinal cord (data not shown; Browne et al., 2001). Overall, data suggest an important role for metabolic dysfunction in the etiology of the motor neuron disease in this mouse model of ALS.

Studies Additional to SOW Performed in Year 1: Aconitase enzyme activity in *Hdh* HD mouse brain (Objective #2).

YEAR 2

Objective #5: **To investigate the effects of increasing CAG repeat number on local rates of cerebral glucose use ($lCMR_{glc}$) in a mouse model of HD expressing expanded CAG repeats in murine *HD*: *Hdh* knock-in mice (7, 48 and 90 CAG repeats).**

Cerebral metabolic rates for glucose in *Hdh* mice expressing 50 glutamines, both homozygous and heterozygous for the transgene (Hdh^{Q50}, 48/48 and 48/7 CAG repeats, respectively) were reported in the Year One. Here we report the results of [^{14}C]-2-deoxyglucose *in vivo* autoradiography in four month-old $\boldsymbol{Hdh^{Q92}}$ knock-in mice expressing 90 CAG repeats (equivalent to 92 glutamines, 92Q; 90/90 and 90/7 CAG repeats) to determine:

- if energy metabolism is altered by expression of expanded polyglutamines in huntingtin protein,
- the effect of increased CAG repeat number (90 versus 48, assessed in year 1); and
- the effect of gene dosage on glucose use (heterozygous 90/7 versus homozygous 90/90 mice), at a time point preceding the onset of any behavioral changes and neuronal intranuclear inclusion (NII) formation in these mice.

Animals: Experiments employed 21 mice in three groups: *Hdh* mice both homozygous and heterozygous for the transgene, expressing 92 (Hdh^{Q92}) glutamines (90/90 and 90/7 CAG repeats, respectively) and in normal wild-type littermates (Hdh^{Q7}, 7/7 CAGs). Two mice were excluded from the 2-DG procedure analysis due to abnormal glucose or blood gas levels.

Physiological Variables: Arterial plasma glucose concentration, *p*O2, *p*CO2 and *p*H were measured 35 minutes into the procedure (10 minutes before animal decapitation) to determine the physiological status of the animals. There were no significant differences in the levels of any of these measured parameters between 7/7 wild type mice and levels in 90/7 and 90/90 mice ($p > 0.05$, ANOVA, followed by Fisher's PLSD). All measured parameters were within accepted normal ranges, indicating that there are no physiological effects associated with the *Hdh* mutation that might alter the interpretation of glucose use results.

Glucose Utilization: Glucose use values in 21 brain regions examined are presented in Table 6. A comparison of glucose use values between Hdh^{Q92} and Hdh^{Q50} mice is shown in Figure 4. Glucose use values were markedly increased throughout the brains of 90/90 Hdh^{Q92} mice. Increases reached statistical significance in 15 of the 21 regions examined, and were not restricted to brain regions susceptible to degeneration in HD (ie. striatum, cortex). Furthermore, glucose use levels in 90/90 mice were significantly elevated over levels in 90/7 mice in 3 regions, suggesting a potential gene dosage effect, as well as a CAG length-dependent effect (see Figure 4).

Discussion: We previously found that glucose use rates did not significantly differ between Hdh^{Q50} and Hdh^{Q7} mice in any of the brain regions examined ($p > 0.05$; ANOVA, followed by Fisher's PLSD), and there was no effect of gene dosage in Hdh^{Q50} mice (48/48 vs 48/7). In this study, we found

Table 6: Local Cerebral Glucose Utilization ($lCMR_{glc}$) in *Hdh* ^{Q92} CAG Knock-in Mice

REGION	7/7	90/7	90/90
Frontal Cortex	52.3 ± 6.6	60.1 ± 3.6	78.2 ± 6.7 ** †
Parietal Cortex	50.0 ± 7.0	58.5 ± 4.0	75.3 ± 7.6 *
Anterior Cingulate Cortex	74.2 ± 11.8	78.4 ± 7.3	99.2 ± 8.7
Auditory Cortex	51.0 ± 6.0	64.9 ± 5.4	81.5 ± 8.7 *
Striatum: Dorsolateral	57.8 ± 7.1	61.5 ± 5.9	81.1 ± 6.2 * †
Ventromedial	55.8 ± 7.3	58.1 ± 6.1	76.0 ± 6.7
Globus Pallidus	32.3 ± 4.1	38.3 ± 2.5	50.3 ± 7.8 *
Hippocampus: CA1	30.0 ± 4.1	41.3 ± 3.6	50.3 ± 6.9 *
CA3	41.2 ± 5.4	52.7 ± 3.4	66.3 ± 9.6 *
Dentate Gyrus: Molecular Layer	47.7 ± 6.1	55.8 ± 4.6	73.2 ± 6.0 ** †
Dorsolateral Geniculate Body	49.0 ± 6.6	56.9 ± 4.8	71.5 ± 10.1
Medial Geniculate Body	56.8 ± 7.2	67.2 ± 3.7	75.0 ± 9.2
Superior Colliculus: Superficial Layer	46.8 ± 6.1	54.9 ± 4.5	68.2 ± 6.8 *
Deep Layer	46.2 ± 6.1	55.1 ± 3.3	68.1 ± 6.3 *
Internal Capsule	12.4 ± 1.7	18.6 ± 1.2	24.2 ± 6.6 *
Thalamus: Dorsomedial	54.7 ± 8.0	65.6 ± 4.4	84.3 ± 10.2*
Ventromedial	39.6 ± 5.9	47.3 ± 4.0	58.3 ± 7.9 *
Substantia Nigra: *pars reticulata*	28.6 ± 4.0	37.4 ± 2.0	44.1 ± 6.5 *
pars compacta	48.5 ± 7.7	58.5 ± 4.3	69.7 ± 11.2
Cerebellum: Grey matter	31.0 ± 4.2	37.0 ± 2.4	47.5 ± 7.5 *
White matter	21.2 ± 2.3	27.7 ± 1.8	29.8 ± 4.6

$lCMR_{glc}$ (nmol/100g/min) in homozygous (90/90) and heterozygous (90/7) *Hdh*^{Q92} knock-in mice; and wild-type (7/7; *Hdh*^{Q7}) littermate controls. Data presented as mean ± SEM, (n=4-6 per group).
* $P < 0.05$, ** $P < 0.01$ relative to levels in 7/7 mice; † $P < 0.05$ relative to 90/7 mice (ANOVA, followed by Fisher's PLSD).

marked increases in glucose use throughout the brains of 90/90 *Hdh*^{Q92} mice. Increases were significant in 15 of the 21 regions examined. Furthermore, glucose use levels in 90/90 mice were significantly elevated over levels in 90/7 mice in 3 regions, suggesting a potential gene dosage effect, as well as a CAG length-dependent effect (see Figure 4). Recent observations suggest that the rate and extent of huntingtin protein translocation from cytosol to the nucleus, and the formation of nuclear huntingtin aggregates, increase with higher CAG repeat lengths (Wheeler et al., 2000, 2002). Therefore, there is reason to suppose that any energetic changes associated with the huntingtin mutation may also vary in time of onset and extent according to the length of the CAG repeat. We are currently investigating this hypothesis further in *Hdh*^{Q111} mice.

The observation that glucose uptake is increased in multiple forebrain regions as a consequence of the gene mutation in *Hdh*^{Q92} mice may at first seem counter-intuitive. We hypothesize that this reflects increased glucose uptake in an attempt to drive metabolism and overcome a metabolic stress in these animals. The fact that *Hdh*^{Q92} mice do not develop overt signs of motor dysfunction or cell loss in their lifetime suggests that in this case the enhanced glucose uptake is sufficient to maintain required ATP production (however, *Hdh*^{Q92} mice do develop nuclear huntingtin aggregates by 15 months of age, Wheeler et al., 2000). The exact nature of any metabolic stress (eg. glycolytic or mitochondrial) has yet to be elucidated. In contrast, *Hdh*^{Q111} mice develop motor abnormalities by approximately

months of age. It will be of interest to compare the time course and magnitude of metabolic abnormalities between *Hdh*^{Q92} and *Hdh*^{Q111} mice.

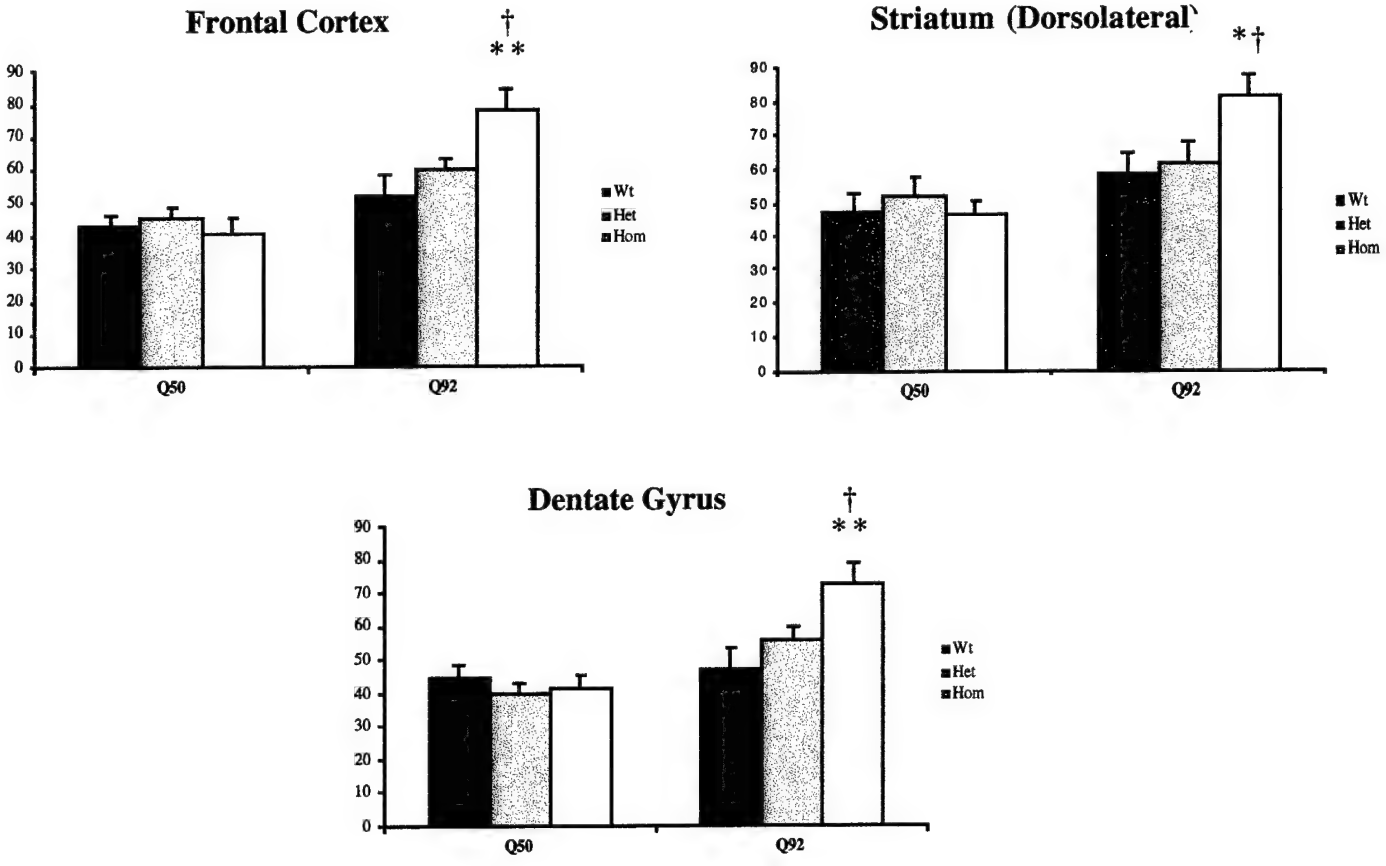

Figure 4: Cerebral Glucose Use in Representative Regions From *Hdh*^{Q50} and *Hdh*^{Q92} Mice

lCMR$_{glc}$ (nmol/100g/min) in 4 month-old *Hdh*^{Q50} and *Hdh*^{Q92} homozygous (Hom) and heterozygote (Het) mice, and wild-type (Wt, 7/7) littermate controls. Data presented as mean ± SEM, (n=6 per group).* $P < 0.05$, ** $P < 0.01$ relative to levels in 7/7 mice; † $P < 0.05$ relative to 90/7 mice (ANOVA, followed by Fisher's PLSD).

Objective #6: **To determine if glucose use is altered over the life-span of a transgenic HD mouse model expressing a human mutant HD fragment: R6/2 HD mice.**

In the original grant protocol we proposed measuring cerebral glucose utilization throughout the brains of HD transgenic R6/2 mice, both prior and after symptom onset (at around 8 weeks), to determine if energetic defects play a causative role in disease pathogenesis. Subsequent to award of this grant, we found that R6/2 mutant mice develop a diabetic profile from approximately 7 weeks of age (Ferrante et al., 2000). Mice show elevated basal blood plasma glucose levels (>> 300mg/dL, relative to 150 mg/dL in physiologically normal mice), and reduced glucose tolerance. Elevated baseline plasma levels, outside of a range considered physiologically "normal" (5-16mM / 91-290mg/dL in rodents), confounds use of the [^{14}C]-2-deoxyglucose technique (Sokoloff et al., 1977).

This *in vivo* imaging procedure utilizes an 'operational equation' to extrapolate rates of glucose utilization in a given brain region from measured parameters, which include levels of circulating arterial plasma glucose, rate of uptake of injected tracer [^{14}C]-2-deoxyglucose from the circulating blood, and detected levels of [^{14}C] in the brain region of interest at the end of the experiment. The equation also relies on assumed kinetic rate constants for blood-brain transfer of glucose and 2-deoxyglucose, which are based on levels measured in rodents under physiologically "normal" conditions. Outside of these conditions, the kinetic constants used in the operational equation no longer apply and any extrapolated results become unreliable (Sokoloff et al., 1977). Consequently, we have been unable to perform glucose use studies in R6/2 mice due to their basal and stress-induced hyperglycemia. We explored measuring glucose use levels in mice before they develop the diabetic profile (4-6 weeks of age), but studies in mice this young are confounded by their small size, which makes surgical preparation of the animals extremely difficult and increases stress in the mice.

In lieu of studies in R6/2 mice, we employed another mutant mouse model of HD expressing an N-terminal fragment of human mutant huntingtin, N171-82Q mice with an 82-polyglutamine expansion (Schilling et al., 1999). N171-82Q mice develop a relatively rapid disease phenotype characterized by onset of motor abnormalities, nuclear huntingtin aggregate (NII) deposition, and striatal-specific neuronal loss by 3-4 months of age. Mice generally live 4-5 months, and develop a diabetic profile by 3.5-4 months of age. We carried out studies to identify whether metabolic abnormalities are present in mutant N171-82Q mice at 2 months of age, prior to huntingtin aggregate formation, striatal cell loss, behavioral and diabetic phenotype in this model. This time point was chosen to determine if energetic changes play an early role in the disease. Results were compared with levels in wildtype (Wt) littermates, and in control mice expressing the human transgene with a non-mutant length polyglutamine expansion, N171-18Q. Results are discussed below.

[^{14}C]-2-Deoxyglucose Measures of Cerebral Glucose Use in N171-82Q HD Mice.

Animals: We measured cerebral glucose use rates in conscious N171-82Q mutant mice, N171-18Q transgenic control mice, and non-transgenic wild-type littermate mice at 2 months of age. In the Year 2 progress report we reported glucose use values obtained in eleven mice to that date. (Experiments were conducted in 18 mice, but seven were excluded due to plasma glucose levels out of normal physiological ranges, abnormal blood gas levels, or poor perfusion of radionuclide. A further eight mice died during the surgery or procedure, or had insufficient blood flow in their femoral catheters). Year 2 results suggested differences between groups may be being masked by variance within groups and small group size. Therefore, in the third year of this project we extended group sizes to numbers estimated by Power Analysis (from Year 2 data) to be adequate to detect inter-group differences. Here we report the cumulative data from years 2 and 3. In the third year of this project, we extended studies by conducting further 2-DG experiments in 20 additional two month-old N171-82Q, -18Q and wildtype mice. (Eight mice were excluded from the final evaluation due to deaths during the

surgery/procedure, or insufficient arterial or venous blood flow rates; 1 was excluded on the basis of abnormally high arterial plasma glucose levels; 6 were excluded due to insufficient radionuclide perfusion).

***Physiological Variables*:** Mice require 1.5-2h for anesthetic clearance from the brain after surgery. Wild type control and N171-18Q mouse basal arterial glucose levels were normal by 2h after surgery (~150 mg/dL). In contrast, N171-82Q mice required 4-5 hours recovery after anesthesia for their basal glucose levels to return from elevated to approaching normal levels. This is likely due to an inability to buffer anesthesia stress-induced glucose upregulation, although mice are not overtly diabetic at this time point. At the time of the experiment, glucose values in N171-82Q mice were elevated relative to control levels (183 ± 22 vs 155 ± 8 mg/dL), but were within the physiologic "normal" constraints of the procedure. Arterial plasma levels did not alter over the time course of the procedure, indicating that mice were not stressed by the technique. Arterial pO_2, pCO_2 and pH values measured at the end of the 45min 2-DG procedure did not differ between groups and were well within "normal" physiologic ranges for mice. Data are presented in Table 7.

	Wildtype	N171-18Q	N171-82Q
Pre-Glucose (mg/dL)	155.0 ± 8.0	168.7 ± 14.4	182.8 ± 21.9
Glucose + 45 min. (mg/dL)	150.5 ± 5.5	201.3 ± 19.7	174.4 ± 10.7
p_aO_2 (mm Hg)	110.0 ± 9.0	38.7 ± 7.8	121.4 ± 8.6
p_aCO_2 (mm Hg)	40.5 ± 1.7	37.5 ± 3.4	38.8 ± 2.4
pH	7.32 ± 0.03	7.31 ± 0.01	7.36 ± 0.01*
Number of animals	4	7_a	5

TABLE 7: Data presented as mean ± SEM for: arterial plasma glucose concentrations measured immediately before [^{14}C]-2-deoxyglucose isotope injection (Pre-Glucose) and at the end of the 2-DG procedure (Glucose + 45 min); and arterial blood gas levels at the end of the procedure. * $p<0.05$, significant difference relative to N171-18Q mice (ANOVA, followed by Fisher's PLSD post-hoc unpaired t-test). a: p_aCO_2 data only available for 6 N171-18Q mice. Arterial plasma glucose levels did not alter significantly over the 45 min duration of the experiment in any group ($p> 0.05$, Student's paired t-test).

Cerebral Glucose Use ($lCMR_{glc}$): Local cerebral rates of glucose use in N171-82Q mutant mice were significantly elevated in 20 of the 32 forebrain regions examined, relative to levels in wildtype and N171-18Q transgenic control mice,. Rates were unaltered in all five cerebellar regions investigated. Results are presented in Tables 8-10. Figure 5 demonstrates the nature of glucose use changes in 10 representative regions. Glucose use changes were not restricted to regions vulnerable to cell loss in HD (ie. striatum), but occurred in multiple forebrain regions including striatum, all eleven cortex regions examined, auditory, visual and extrapyramidal regions.

Table 8: CORTICAL REGIONS

Region	Wildtype	N171-18Q	N171-82Q
Pre-Frontal: Layers I-III	55.7 ± 8.8	57.1 ± 4.0	72.0 ± 1.5 * †
Pre-Frontal: Layer IV	59.3 ± 10.0	62.4 ± 5.1	78.5 ± 1.1 *
Pre-Frontal: Layers V-VI	49.7 ± 5.0	51.7 ± 3.9	64.7 ± 2.4 *
Frontal: Layers I-III	59.9 ± 7.7	55.1 ± 3.7	68.8 ± 3.9 *
Frontal: Layer IV	59.5 ± 6.3	61.2 ± 3.9	85.2 ± 2.6 ** †
Frontal: Layers V-VI	50.9 ± 4.4	49.5 ± 3.4	65.3 ± 3.0 **
Parietal: Layers I-III	56.5 ± 7.6	47.9 ± 3.9	69.0 ± 3.8 **
Parietal: Layer IV	59.4 ± 9.7	55.1 ± 4.5	80.0 ± 2.5 ** †
Parietal: Layers V-VI	52.5 ± 7.1	50.5 ± 3.7	68.8 ± 2.3 ** †
Anterior cingulate	65.6 ± 10.9	61.2 ± 5.5	85.2 ± 4.2 **
Posterior cingulate	74.0 ± 5.6	74.9 ± 7.5	96.5 ± 4.4 *

Table 9: LIMBIC AND EXTRAPYRAMIDAL REGIONS

Region	Wildtype	N171-18Q	N171-82Q
Striatum:			
Dorsomedial	61.3 ± 7.2	63.9 ± 5.3	72.9 ± 4.0
Dorsolateral	68.8 ± 7.3	73.1 ± 4.0	80.4 ± 2.4
Ventromedial	64.3 ± 5.4	60.4 ± 4.6	77.5 ± 3.3 *
Globus Pallidus	37.2 ± 3.5	39.7 ± 4.0	49.1 ± 2.0
Hippocampus:			
CA1	31.9 ± 5.6	32.4 ± 2.7	42.1 ± 3.5 *
CA3	40.4 ± 6.2	40.9 ± 4.2	50.7 ± 2.6
Dentate gyrus	50.8 ± 7.4	47.1 ± 3.3	61.8 ± 3.1 *
Lateral habenular nucleus	48.7 ± 9.4	67.4 ± 9.5	67.3 ± 7.0
Subthalamic nucleus	63.6 ± 11.1	60.0 ± 5.5	69.3 ± 2.0
Mammilary body	94.0 ± 22.8	88.0 ± 4.0	101.1 ± 6.2
Substantia nigra:			
pars compacta	59.0 ± 6.6	52.3 ± 1.9	64.7 ± 3.6 **
pars reticulata	37.4 ± 7.3	34.1 ± 2.7	42.9 ± 2.5
Cerebellar nucleus	87.0 ± 4.5	91.1 ± 3.6	117.4 ± 9.0 ** †
Cerebellar hemisphere			
granular layer	29.9 ± 3.1	34.5 ± 2.1	37.0 ± 2.1
molecular layer	41.5 ± 4.6	47.5 ± 2.2	52.8 ± 2.4 †
Inferior olive	75.3 ± 12.8	65.2 ± 1.6	73.2 ± 2.9
Cerebellar white matter	24.8 ± 4.3	22.8 ± 1.5	26.8 ± 2.6

Table 10: AUDITORY AND VISUAL REGIONS

Region	Wildtype	N171-18Q	N171-82Q
Visual Regions -			
Visual Cortex: Layer IV	57.1 ± 3.5	62.2 ± 2.1	66.3 ± 5.5
Lateral geniculate body	57.0 ± 7.5	53.7 ± 2.7	62.1 ± 2.4
Superior colliculus:			
Superficial layer	54.2 ± 7.9	54.7 ± 4.5	57.3 ± 2.4
Deep layer	54.9 ± 6.9	53.1 ± 3.2	61.4 ± 2.1
Auditory Regions -			
Auditory Cortex: Layer IV	102.5 ± 4.1	84.5 ± 5.3	105.5 ± 9.1 *
Inferior colliculus	145.3 ± 13.6	125.1 ± 3.0	144.6 ± 18.4
Superior olive	90.0 ± 6.6	85.6 ± 4.0	103.3 ± 8.0 *
Medial geniculate body	81.3 ± 6.5	75.4 ± 3.1	89.4 ± 3.2 *
Cochlear nucleus	87.8 ± 11.1	83.6 ± 3.6	109.1 ± 7.7 **

Local cerebral metabolic rates for glucose (nmol/100g/min) in heterozygous N171-82Q mutant mice (n=5), compared with rates in wild-type littermate controls (n=4), and in heterozygous N171-18Q transgenic controls (n = 7).
*$p < 0.05$, relative to levels in wt mice; † $p < 0.05$ relative to levels in 18Q mice (ANOVA & Fischer's PLSD).

Discussion: The finding of elevated cerebral glucose use levels in N171-82Q mice at an age preceding overt symptomatic or pathologic changes, further supports the hypothesis that metabolic alterations are an early component of events leading to cell dysfunction in HD models. We are currently analyzing results in 3 month-old N171-82Q mice to determine if the magnitude and/or distribution of glucose use changes alters as phenotype is expressed in these mice. (Interpretation of glucose use changes in N171-82Q mice older than 3 months is restricted because mice become diabetic around this age). The next step is to ascertain what these elevations in glucose uptake represent. Increased glucose use may reflect a compensatory effort by cells to overcome a metabolic insult by increasing glycolytic generation of ATP, or by increasing substrate influx into mitochondria. Spectrophotometric enzyme activity assays in brain tissue from cortex, striatum and cerebellum demonstrated no significant differences between maximal enzyme activities in mutant 82Q mice and control groups at 3 months of age (data not shown; Browne et al., unpublished obseravtions). This observation suggests that impaired activity of these enzymes is not responsible for the earlier increases in glucose uptake observed. We are performing *in vitro* studies to determine if mitochondrial uncoupling occurs in these mice by measuring brain ATP levels, mitochondrial ATP synthesis and oxygen consumption rates.

We hypothesize that up-regulation of glucose uptake by neurons may occur early in the lifespan of HD mouse models, to compensate for impairments in other constituents of metabolic pathways. The increased glucose uptake observed in Hdh^{Q92} mice (discussed previously) may be sufficient to prevent cell degeneration in these animals (at least during their 2-year lifespan), but may not be sufficient to prevent neuronal dysfunction in N171-82Q mice. Increases in glucose use appear in multiple forebrain

regions in these models. This does not explain the regional selectivity of cell death seen in HD. One potential explanation is that striatal neurons exhibit an increased vulnerability to metabolic impairments relative to other neuronal populations. This suggestion is supported by observations that striatal cells are particularly vulnerable to mitochondrial toxins (eg. 3-NP, azide), metabolic insults (eg. ischemia), and excitotoxins (eg. quinolinic acid), in addition to the substantial glutamatergic input to the striatum from the cortex.

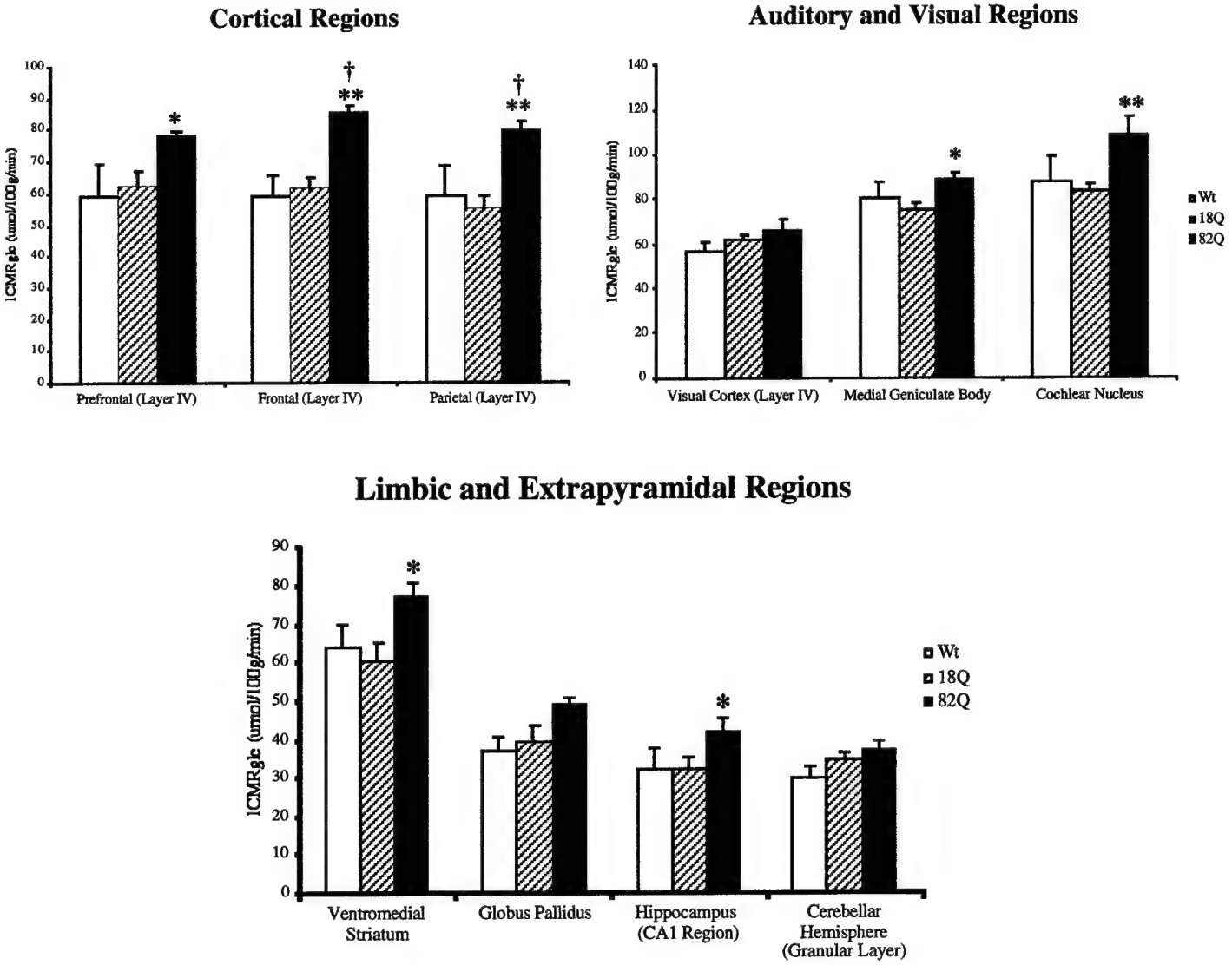

Fig 4: Local cerebral metabolic rates for glucose (nmol/100g/min, mean ± SEM) in heterozygous N171-82Q mutant mice, compared with rates in wildtype littermate controls (Wt), and in heterozygous N171-18Q transgenic controls. *$p < 0.05$, relative to levels in Wt mice; † $p < 0.05$ relative to levels in N171-18Q mice (ANOVA & Fischer's PLSD). N = 4-7 per group.

Objective #7: **Measurement of electron transport chain enzyme activities in R6/2 HD mice, before and after symptom onset and pathological changes.**

There are multiple reports of metabolic enzyme dysfunction in HD post-mortem brain, notably reduced complex II-III, IV, and aconitase activities localized to caudate and putamen (Browne et al., 1997; Gu et al., 1996). We used spectrophotometric assays to measure mitochondrial metabolic enzyme activities in brains from R6/2 HD mice.

Animals:. Whole forebrain and cerebellum homogenates were prepared from frozen brain tissue taken from R6/2 mice at 3.5, 8 and 12 weeks of age. Enzyme activities measured were glyceraldehyde-3-phosphate dehydrogenase (GAPDH; glycolytic enzyme); aconitase and citrate synthase (Kreb's cycle enzymes); complexes I, II-III and IV of the mitochondrial electron transport chain. Complex enzyme activities (per mg protein) were corrected by the citrate synthase activity (per mg protein; a mitochondrial matrix enzyme) as a correction for differential mitochondrial number between preparations. Results are shown in Table 11. No alterations in activities of any of the enzymes measured were detected in whole brain homogenates from 3.5 and 8 week-old mice. Increased complex I and II-III activities were detected in R6/2 forebrain at 12 weeks of age. GAPDH activity was significantly elevated in the cerebellum of 12 week-old R6/2 mice relative to wild type littermate control levels. Aconitase activity was unaltered in all regions at all time-points (data not shown).

		FOREBRAIN		CEREBELLUM	
		Wt	R6/2	Wt	R6/2
Complex I: (/CS)	3 wk	0.14 ± 0.02	0.16 ± 0.01	0.17 ± 0.03	0.13 ± 0.03
	8 wk	0.11 ± 0.01	0.12 ± 0.02	0.13 ± 0.02	0.14 ± 0.02
	12 wk	0.10 ± 0.01	0.14 ± 0.02 *	0.15 ± 0.02	0.16 ± 0.02
Complex II-III: (/CS)	3 wk	0.19 ± 0.02	0.19 ± 0.03	0.20 ± 0.03	0.20 ± 0.02
	8 wk	0.13 ± 0.01	0.15 ± 0.02	0.13 ± 0.01	0.16 ± 0.03
	12 wk	0.13 ± 0.01	0.18 ± 0.02 *	0.15 ± 0.01	0.14 ± 0.01
Complex IV: (/CS)	3 wk	1.24 ± 0.21	1.46 ± 0.16	1.26 ± 0.17	1.35 ± 0.13
	8 wk	0.88 ± 0.16	0.85 ± 0.13	0.85 ± 0.09	0.98 ± 0.29
	12 wk	1.09 ± 0.17	1.25 ± 0.16	1.20 ± 0.22	1.13 ± 0.13
GAPDH: (/mg prot.)	3 wk	1.26 ± 0.06	1.45 ± 0.14	1.24 ± 0.14	1.26 ± 0.10
	8 wk	2.84 ± 0.22	2.61 ± 0.16	1.72 ± 0.26	1.68 ± 0.21
	12 wk	2.67 ± 0.30	3.12 ± 0.20	1.91 ± 0.21	2.65 ± 0.33 *

Table 11: Metabolic Enzyme Activites Over the Lifespan of R6/2 HD Mice

Data are mean ± SEM citrate synthase (CS)-corrected enzyme activities (nmol/min/mg protein/CS) in forebrain and cerebellun from R6/2 and wildtype littermate (Wt) mice. Measurements were made at 3 (n=5-6), 8 (n=5-6) and 12 (n=10 per group) week of age. * $p < 0.05$, significant difference relative to wild type control mice (ANOVA, with post-hoc Fisher PLSD).

Discussion: Activities of all enzymes measured were unaltered in both forebrain and cerebellum homogenate preparations before symptom onset (3.5 and 8 weeks of age). Increases in complex I and II-III activities in forebrain, and GAPDH in cerebellum, were evident in symptomatic 12 week-old mice. We found no enzymatic abnormalities in mice at 3 or 8 weeks of age, suggesting that any alterations in these metabolic enzymes occur only after symptom onset. Our findings differ from one previous report which shows reduced complex II-III activity and markedly decreased aconitase activity in forebrain from 12 week-old R6/2 mice (Tabrizi et al., 2000). However, another report found no difference in oxidative phoshorylation enzyme activities in R6/2 striatum and cerebral cortex (Guidetti et al., 2001). Reasons for these discrepancies are not obvious, however the bulk of evidence seems to suggest that mitochondrial enzyme activities are not significantly impaired up to 12 weeks of age in R6/2 mouse forebrain. Our results also suggest that reductions in complex II-III and IV, and aconitase activities in affected brain regions (caudate and putamen) of symptomatic, end-stage (grade 3 and 4) HD patients are not replicated in the R6/2 model (Browne et al., 1997; Gu et al., 1997; Tabrizi et al., 1999). This latter observation may indicate that the pathophysiology of the R6/2 model differs from HD pathogenesis in humans. Alternatively, the rapid time-course of the disorder in mouse models may preclude the development of metabolic enzyme alterations. In support of this, a recent study by Guidetti and colleagues (2001) found no significant alterations in aconitase or oxidative phosphorylation enzyme activities in early stage HD patients (grade 0 and 1), suggesting that mitochondrial enzyme perturbations are secondary consequences of the disease process. Alternatively, region-specific alterations in brain regions vulnerable to damage in HD (ie. the caudate and putamen in human, analagous to striatum in rodents), may be masked by the use of whole forebrain homogenate preparations in this study. Investigations in specific brain regions in R6/2 mice were precluded in Year 2 of this project, due to the large numbers of mice required to gather sufficient striatal tissue. Subsequently, in light of Guidetti and colleagues report that they found no enzymatic changes in cortex and striatum of R6/2 mice (Guidetti et al., 2001), we chose not to pursue further studies in this model. We did, however, measure oxidative phopshorylation enzyme activities in three different brain regions of N171-82Q HD mice (data not shown). Results in three month-old symptomatic N171-82Q mice showed no significant alterations in complex II-III, complex IV, or citrate synthase activities in striatum, cerebral cortex, or cerebellum, relative to levels in N171-18Q controls and wildtype littermates (n=20-30 per group) (Browne et al., unpublished observations). This finding further supports the suggestion that alterations in oxidative phosphorylation enzyme activities that are implicated in HD in humans, do not play a causative role in the disease phenotype in mutant mouse models of HD.

Objective #8. **NMR assessment of cerebral lactate levels in *Hdh* and R6/2 mice.**

Increased lactate production is a marker for metabolic dysfunction, putatively indicating elevated glycolytic activity, or pyruvate shunt to form lactate rather than entering mitochondrial metabolic

pathways. Lactate levels in brain can be measured non-invasively *in vivo* by NMR spectroscopy. Studies were performed during Year 2, and data analysis completed in Year 3 of this project.

Animals: We carried out NMR spectroscopic measurements of lactate and metabolite levels in the basal ganglia of anesthetized R6/2 and wildtype littermate mice at 12 weeks of age (n = 5 per group).

Lactate Levels: Lactate levels were calculated as the ratio of lactate to creatine, which we have previously shown to be unaltered in the basal ganglia of R6/2 mice (Ferrante et al., 2000). Results show increased lactate levels in the basal ganglia of R6/2 mice compared with levels in wildtype littermates (Figure 5). The average lactate level in R6/2 mice was 0.14 ± 0.06 (ratio, mean ± SEM), and was unobservable (and hence not quantifiable) in the wildtype mice (evident from Figure 5, which shows the averaged spectra for 5 R6/2 mice and 5 wildtype mice).

Discussion: Results suggest that lactate production in basal ganglia is elevated in symptomatic R6/2 mice, compared with age-matched wildtypes in which basal lactate levels were generally undetectable from background levels. Studies should be expanded to multiple time-points to determine whether abnormalities in lactate production occur before symptomatic and pathologic changes in this mouse model of HD.

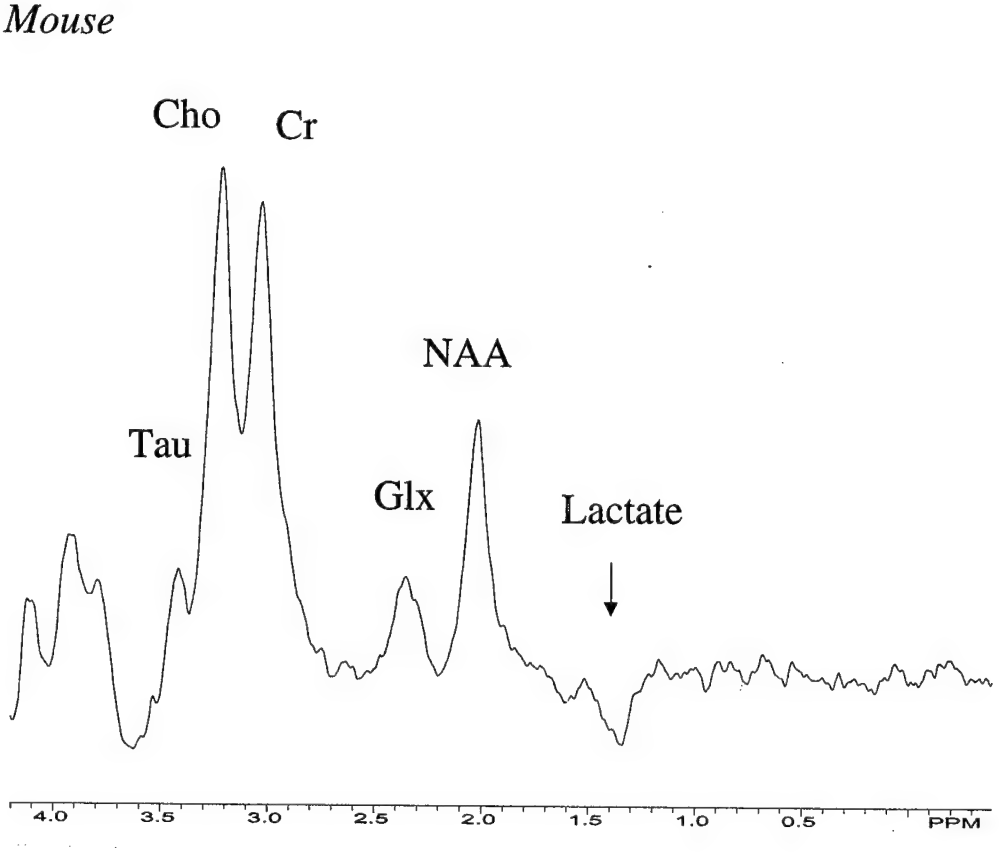

Figure 5: Averaged NMR spectra from basal ganglia of12 week old R6/2 and wildtype (WT) mice (n=5).
Abbreviations: Cho, choline; Cre, creatine; Glx, glutamine; NAA, N-acetylaspartate; Tau, taurine.

Year 3:

***Objective #9.* Assessment of oxidative damage markers in *Hdh* and R6/2 mice.**

In the original specific aims of this project we aimed to use HPLC to measure four different markers of oxidative damage in brain of R6/2 and *Hdh* mouse models of HD. These were protein carbonyls, nDNA OH^8dG; hydroxyl radical production and nitrotyrosine levels. We have encountered problems with measurement of two of these markers, nitrotyrosine and protein carbonyls. Despite a great deal of effort to re-instate reliable HPLC detection of nitrotyrosine using Coullarray electro-chemical detection (ESA, Chelmsford MA) following our laboratory's move, we have been unable to reproducibly detect basal nitrotyrosine in mouse brain at levels above background noise. This project has consumed several months of work, but unfortunately yielded no results. We are now pursuing immunohistochemical detection of nitrotyrosine in these HD models (previously reported in R6/2 mice; Perez-Severiano *et al.*, 2000; Tabrizi *et al.*, 2000).

Similarly, the laborious and time-consuming protein carbonyl HPLC assay has not generated reproducible data in HD mouse brain. Therefore, we have recently developed a western blot assay for carbonyl levels. Assays in HD mice are still in progress.

We have, however, successfully measured levels of the DNA damage product 8-hydroxy-deoxyguanosine (OH^8dG) in nuclear brain extracts of R6/2 mice. We have also developed technology to measure OH^8dG levels in body fluids, including plasma and urine. We have successfully measured levels of hydroxyl radical production in the N171-82Q HD mice (which resemble the R6/2 model). We have also extended studies to examine levels of the lipid oxidative damage markers, malondialdehyde, acrolein, 8-iso-prostaglandin F2 and 4-hydroxynonenal by immuno-histochemical techniques (in lieu of the lack of carbonyl and nitrotyrosine data). Results are presented below.

a) Oxidative Damage Studies: OH^8dG in R6/2 Mouse Urine, Plasma, DNA and Brain Tissue

We examined free OH^8dG levels in urine, plasma and striatal microdialysates and DNA OH^8dG levels in cortex and striatum of the R6/2 mice.

Animals: Thirty R6/2 and 29 littermate wildtype mice at 12 weeks of age were used in experiments.

OH^8dG: We found that urine and plasma concentrations of OH^8dG were significantly increased in the R6/2 mice at 12 weeks of age (Table 12). Furthermore we used *in vivo* microdialysis to demonstrate that there were significant increases in extracellular OH^8dG levels in the striatum of the R6/2 mice as compared to age-matched littermate controls (Table 12). We also found that OH^8dG is increased in genomic DNA isolated from the striatum of R6/2 mice (Figure 6). We utilized OH^8dG immunocytochemistry to show an age-dependent increase in staining, consistent with the biochemical measurements (data not shown).

Discussion: These findings provide direct *in vivo* evidence for increased oxidative stress in the brains of the R6/2 mice. Results are consistent with studies showing progressive increases in staining of other oxidative damage markers for lipid peroxidation, and increased 3-nitrotyrosine staining in the R6/2 mice (Perez-Severiano *et al.*, 2000; Tabrizi *et al.*, 2000). Studies are currently being extended to *Hdh* mice.

Table 12: OH^8dG levels in urine, plasma and microdialysates of R6/2 and control mice

	R6/2 (n)	Controls (n)
Urine ng/mg creatinine	18.4 ± 4.99 (10)[a]	6.2 ± 0.7 (10)
Plasma pg/ml	24.8 ± 9.49 (30)[b]	51.6 ± 13.6 (29)
Microdialysates pg/ml	2.8 ± 0.26 (10)[c]	2.0 ± 0.2 (9)

Data are presented as mean ± SEM. [a] p=0.02; [b] p=0.006; [c] p= 0.018 vs. controls. (Group sizes in parentheses)

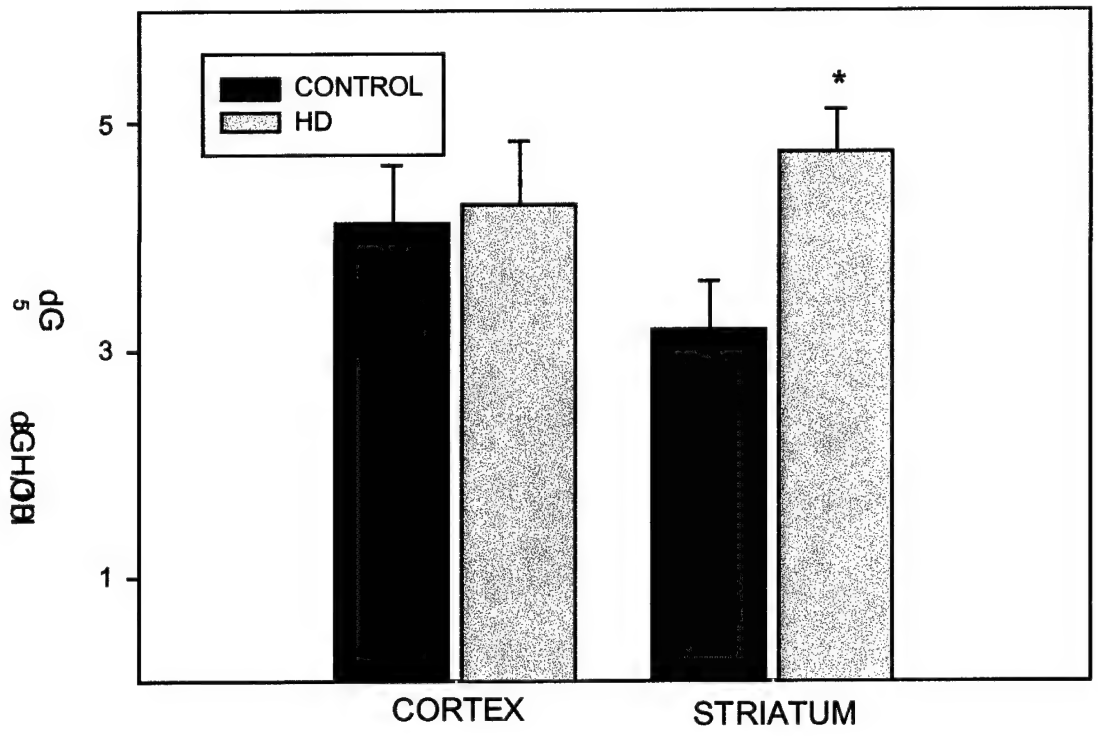

Figure 6: OH^8dG levels in cortex and striatal DNA from R6/2 (HD) and littermate wild-type control mice.
Data are mean ± SEM OH^8dG/dG ratios. * p<0.05 (Student's unpaired t-test).

b) Oxidative Damage Studies: Hydroxyl Radical Generation in N171-82Q Mouse Striatum

In another approach to investigate whether oxidative damage to cellular elements is increased as a result of the HD mutation, we used microdialysis with HPLC to compare the rates of hydroxyl radical formation in striatum from N171-82Q and wild-type mice, both at baseline and following cell stress by exposure to a neurotoxin (3-nitropropionic acid, 3-NP). This technique measures the conversion of 4-hydroxybenzoic acid (4-HBA) to 3,4-dihydroxybenzoic acid (3,4-DHBA) by reaction with endogenous hydroxyl radicals (OH^-), as a measure of "hydroxyl radical-like" production.

Animals: Experiments were performed in symptomatic N171-82Q mice (n=4), N171-18Q "non-HD" mice (n=6) and wild-type littermate control mice (n=6) at 3 months of age (symptomatic). 4-HBA (400 mg/kg i.p. in saline) was administered to mice, and microdialysate samples were collected from the striatum at 20 minute intervals for the subsequent 3 hours. Mice then received 3-NP (100 mg/kg i.p.), and microdialysates were collected every 20 minutes for a further 3 hours. Levels of 3,4-DHBA in the dialysate, formed by the reaction of hydroxyl radicals with 4-HBA, were measured by HPLC detection.

OH^- Generation: Results are presented as the ratio of 3,4-DHBA to 4-HBA accumulated over the 3 hour periods before and after 3-NP administration (Figure 7). Basal levels of hydroxyl radical generation (3,4-DHBA/4-HBA ratio) are higher in N171-82Q mice than in either N171-18Q transgenic controls, or in wildtype littermate mice. Both control groups showed elevated OH^- production in response to 3-NP, whereas N171-82Q mice did not. The reason for this observation is unclear.

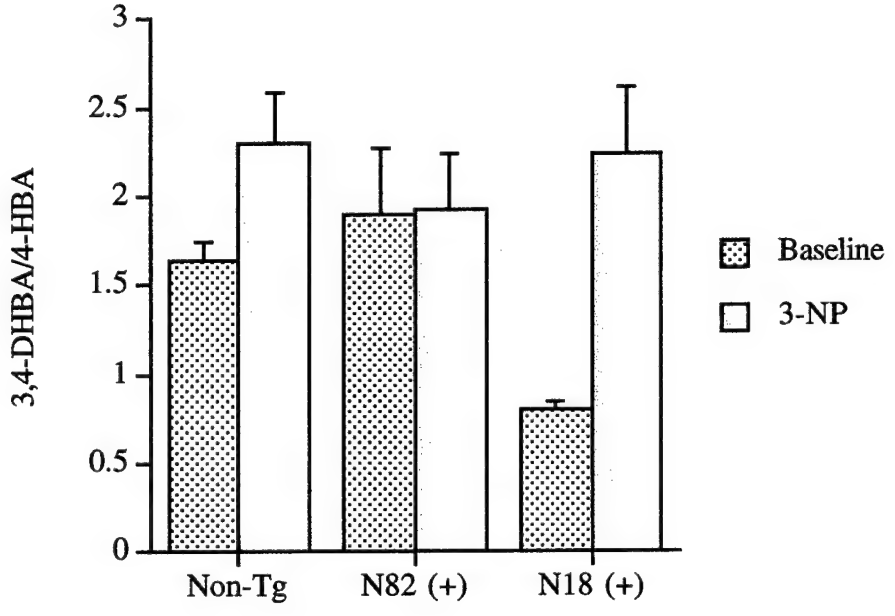

Figure 7: Free Radical Production in N171 HD Mice.

Data are mean ± SD 3,4-DHBA/4-HBA ratios, representative of OH^- radical levels, in 12 week-old mice (baseline), and following stress induced by 3-NP administration (100mg/kg i,p,). Subjects were N171-82Q mutant HD mice (N82+), N171-18Q transgenic controls (N18+), and wildtype littermates (Non-Tg).

Discussion: Results suggest that HD mice exhibit elevated free radical production in the striatum, a brain region vulnerable to cell loss in HD, around the time of symptom onset (3 months of age in N171-82Q mice). This observation adds support to the hypothesis that free radical damage is involved in disease etiology in this mouse model, but further studies of the temporal pattern of radical generation are needed to verify results and to determine if this is a causative event in pathogenesis. We also require studies in other brain regions to determine if this effect is restricted to vulnerable regions in HD (ie. striatum), or is a widespread, non-specific phenomenon. Studies are being extended to *Hdh* mice.

c) Oxidative Damage Studies: Immunohistochemical Studies in R6/2 Brain

We have initiated immunohistochemical studies in R6/2 mice to qualitatively assess expression levels of other markers of oxidative damage to lipid, namely malondialdehyde, acrolein, 8-iso-prostaglandin F2 and 4-hydroxynonenal. Preliminary findings in 12 week-old R6/2 striatum did not reveal any alterations in levels of malondialdehyde amd acrolein, compared with staining levels in wildtype littermates (data not shown). However, 8-iso-prostaglandin F2 and 4-hydroxynonenal staining were both found to be increased in R6/2 mice, relative to wild-type levels, in 12 week-old mice (Figure 8).

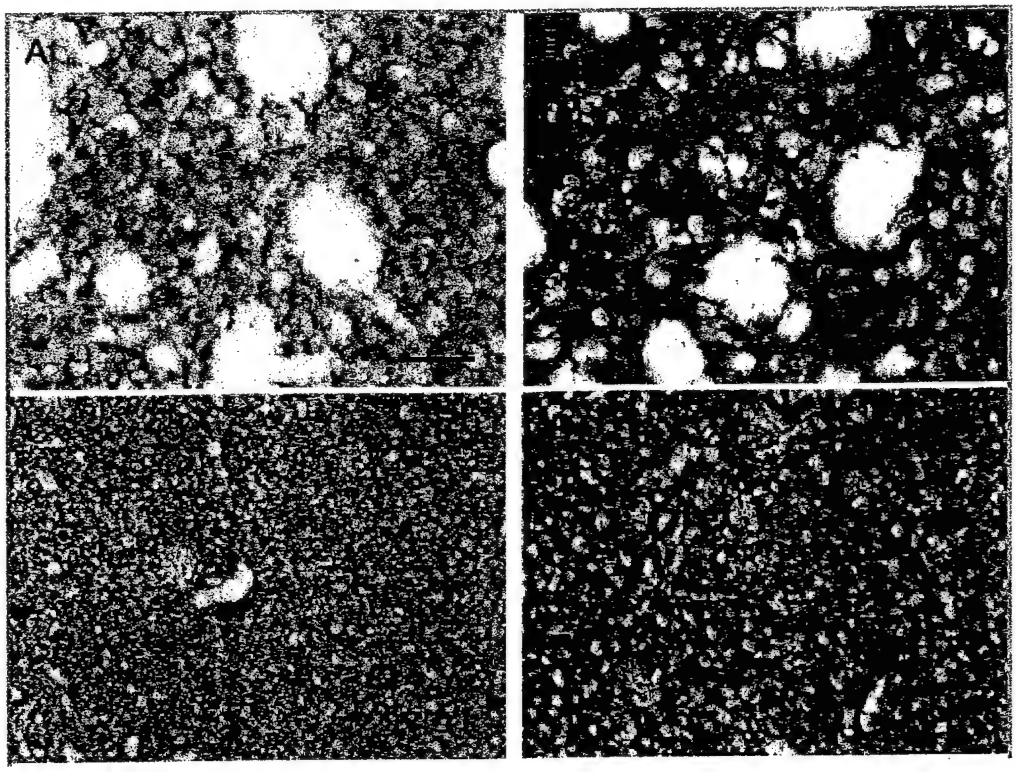

Figure 8: 8-iso-prostaglandin F2 (A, B) and 4-hydroxynonenal (C, D) immunoreactivity in the striatum of wild type (A, C) and R6/2 mice (B, D) showing increased staining in neurons, neuropil and vascular profiles in R6/2 mice. Scale bar = 50 m (A, B), 100 m (C, D).

Objective #10. **Assessment of oxidative damage markers in *G93A ALS Mice*.**

In the original specific aims of this project we aimed to use HPLC to measure four different markers of oxidative damage in G93A mouse CNS: protein carbonyls, nDNA OH^8dG, hydroxyl radical production and nitrotyrosine levels. As discussed in "Objective # 9', we have encountered problems measuring nitrotyrosine levels reproducibly using HPLC techniques. However, elevated nitrotyrosine staining has previously been demonstrated in G93A brain (Ferrante et al., 1997). Therefore, in Year 3 of this project we concentrated on measurements of oxidative damage to protein (protein carbonyl levels) and lipid (malondialdehyde levels).

a) Protein Carbonyl Measures in G93A Mice

Animals: Experiments were carried out in G93A mice and wildtype littermate controls at 90 days of age (immediately prior to symptom onset), 110 days (at symptom onset), and at 130 days (symptomatic, end-stage. (n = 6-8 per group). Measurements were made in tissue from four CNS areas: cerebral cortex, brainstem, cerebellum and spinal cord.

***Results*:** Protein carbonyl levels are presented in Table 13. No differences between G93A and wildtype mice were detected in 90 day-old mice, in any of the regions examined. By 110 days, carbonyl levels were significantly elevated in the spinal cord (+47%) and cerebral cortex (+14%). By 130 days of age, carbonyl levels were further increased in these regions (+80% in spinal cord; +59% in cerebral cortex), but remained unaltered in brainstem and cerebellum.

Table 13: Protein Carbonyl Levels in G93A FALS Mice

	90 Days	110 Days	130 Days
Spinal Cord			
Control	1.05 ± 0.34	0.99 ± 0.06	0.87 ± 0.17
G93A	1.11 ± 0.34	1.46 ± 0.15 *	1.57 ± 0.17 *
Cerebral Cortex			
Control	0.75 ± 0.08	0.71 ± 0.06	0.81 ± 0.05
G93A	0.86 ± 0.13	0.88 ± 0.05 *	1.29 ± 0.12 *
Brainstem			
Control	1.15 ± 0.12	1.14 ± 0.10	1.21 ± 0.11
G93A	1.13 ± 0.30	1.23 ± 0.09	1.19 ± 0.27
Cerebellum			
Control	0.52 ± 0.10	0.70 ± 0.11	0.87 ± 0.07
G93A	0.53 ± 0.10	0.69 ± 0.06	0.97 ± 0.17

Data are mean ± SEM, carbonyls (U/mg protein), n = 6-8 per group.
* $p < 0.01$, relative to wildtype control values (Student's unpaired t-test).

Discussion: Marked elevations in protein carbonyl levels in both spinal cord and cerebral cortex, with sparing in brainstem and cerebellum, suggest that regions vulnerable to degeneration undergo abnormal levels of oxidative damage to proteins in this ALS model. Trends towards increased oxidation are present in pre-symptomatic 90 day old G93A mice, but do not reach statistical significance until the 110 day time-point, around the onset of symptoms. Mice begin to show pathologic changes at approximately 70 days of age (mitochondrial perturbations, Gurney et al., 1995). It is also noteworthy that the extent of carbonyl elevation is greatest in the spinal cord, which is the principal site of neuronal degeneration in the ALS phenotype. However, motor neuron cell bodies and motor association areas in the cortex are also affected in the disease, and also show carbonyl increases in this mouse model of ALS. Results indicate that increased oxidative damage occurs in vulnerable regions during a period between the first pathologic changes and the onset of motor symptoms in the G93A model.

b) Malondialdehyde Levels in G93A Mouse Spinal Cord

Mice: Experiments were carried out in G93A mice and wildtype littermate controls at 30 and 50 days of age (prior to pathologic changes), 70 days (around time of first pathological changes), and 110 days (at symptom onset), 8-19 mice per group. Levels were also measured in transgenic N1029 mice that overexpress human normal SOD1, as controls for the transgene manipulation in the G93A mice, at 70 and 110 days of age (n = 9-10 per group). Measurements were made in spinal cord, since this is the major site of degeneration in the ALS model.

***Results*:** Malondialdehyde levels are presented in Table 14. No significant differences between G93A and wildtype mice, or N1029 control mice, were detected at any time-point investigated.

Discussion: Results show no evidence of oxidative damage to lipid detectable using this technique in G93A spinal cord.

Table 14: Malondialdehyde Levels in Mouse Spinal Cord

Mouse Line	30 Days	50 Days	70 Days	110 Days
G93A	12.4 ± 1.8 n=16	8.67 ± 0.67 n=9	8.18 ± 1.53 n=10	10.88 ± 1.63 n=16
N1029			6.17 ± 2.17 n=9	10.42 ± 1.70 n=10
Wt	10.5 ± 2.4 n=16	8.05 ± 1.40 n=12	6.44 ± 1.33 n=8	9.99 ± 2.41 n=19

Data are mean ± SEM, malondialdehyde levels(nM TBA/mg protein), n = 8-19 per group.
$p > 0.05$, relative to both N1029 and wildtype control values (ANOVA).

Objective #11. **Measurement of Cerebral Metabolite Levels in HD Mouse Brains**

HPLC was used to measure levels of the energy metabolites ATP, ADP, AMP, creatine and phosphocreatine in brain tissue from R6/2 HD mice, according to methods in the original proposal. Studies are currently being carried out in R6/2 mice at younger ages, and in *Hdh* mice.

Animals: Studies in 12 week old mice were performed using brain tissue from R6/2 (n=6) and wildtype littermate mice (n=5).

Results: Metabolite levels in cerebral cortex and cerebellum are presented in Table 15. Results demonstrate that at this time-point, when mice are symptomatic and towards end-stage of their short lifespan, ATP levels in cortex are markedly reduced in forebrain, and to a lesser extent in cerebellum. In contrast to the approximate 3-fold decrease in ATP levels in R6/2s, relative to wildtype mice, levels of all other metabolites measured were significantly increased in the forebrain. ATP, ADP and AMP were not significantly altered in cerebellum, however creatine and phosphocreatine were markedly increased in this region.

Table 15: Energy Metabolite Levels in Cerebral Cortex of End-Stage R6/2 mice

	Forebrain		**Cerebellum**	
	Wildtype n=5	**R6/2** n=6	**Wildtype** n=5	**R6/2** n=6
Creatine	49.40 ± 2.66	68.46 ± 1.56**	55.69 ± 6.00	84.20 ± 7.70 *
Phosphocreatine	15.09 ± 0.57	39.30 ± 2.01**	11.23 ± 1.65	26.44 ± 5.53 *
AMP	2.70 ± 1.14	7.99 ± 0.13**	4.68 ± 0.99	3.90 ± 0.52
ADP	3.14 ± 0.44	5.78 ± 0.30**	3.94 ± 0.83	6.31 ± 0.91
ATP	15.81 ± 1.43	4.65 ± 0.47**	9.29 ± 1.93	5.28 ± 1.18

Data are Mean ± SEM (nmol/mg protein).
**.$P < 0.0005$, *$p < 0.05$ (ANOVA, with Fisher's PLSD post-hoc).

Discussion: Results suggest that generation of ATP is hindered in symptomatic 12 week old mice in forebrain. Elevations in cellular levels of AMP and ADP may reflect an inability to generate ATP in cells, leading to a build up of precursors. Increases in levels of other metabolites, phosphocreatine and creatine, may implicate that at this late stage in the disorder, cells are using alternative energy sources. Alternatively, energy demand in this region may be reduced. Findings of smaller magnitude alterations in metabolite levels in the cerebellum suggest that metabolism in this region is less affected by the R6/2 HD mutation (at this timepoint). Further studies are required to determine the significance of the increase in creatine and phosphocreatine. We are currently extending studies to mice at ages preceding

symptom onset (4 and 7 weeks) and around symptom onset (9 weeks), to determine the temporal profile of events.

Objective #12. **Measurement of the Effects of 3-NP on Local Cerebral Glucose Use in Rats.**

3-Nitropropionic acid (3-NP) is an inhibitor of complex II of the electron transport chain in mitochondria. Systemic administration in multiple species, including humans, non-human primates, rats and mice, results in selective degeneration of the same populations of basal ganglia neurons that are targeted in Huntington's disease, (ie. spiny projection neurons, with relative sparing of aspiny and cholinergic interneurons). Pathologic changes are accompanied by motor abnormalities and cognitive impairment, again resembling HD. In addition, the enzyme targeted by this agent, complex II (succinate dehydrogenase) has been found to have markedly reduced activity in the caudate and putamen of advanced-stage HD patients (Browne wt al., 1997, Gu et al., 1996). Hence, 3-NP is widely used as a neurotoxin model of HD.

The reason for the selective cell death seen in the brain following 3-NP is unclear, especially since systemic administration of 3-NP results in similar levels of 3-NP throughout the brain, and inhibits complex II activity to the same extent throughout the brain (Browne and colleagues, unpublished observations). Histopathologic investigations suggest that the onset of motor impairment closely correlates with the first pathological changes in the striatum I rodent models of 3-NP neurotoxicity. In these studies, we investigated whether bioenergetic changes were evident in the striata of rats treated with 3-NP prior to cell loss and motor impairment in these animals, using [14C]-2-deoxyglucose *in vivo* autoradiography. In the first study we chose a time-point of 3 days post-3-NP treatment commencement, as this time-point preceded histopathologic and motor changes by approximately 1 day. In the same experiment, we also assessed the effects of creatine pre-treatment on glucose use. Creatine has previously been shown to ameliorate cell death induced by 3-NP in rats, possibly by providing an alternative energy supply to cells under energetic stress. The aim of this study was to determine if creatine treatment altered any energetic changes induced by 3-NP treatment at this time-point.

Intraperitoneal injection of 3-NP in rats induces a motor phenotype characterized by initial hindlimb weakness, which rapidly progresses to hindlimb paralysis and death ensues, generally within 24 to 36 hours after the first observations of paralysis. The time-course of this phenotype is dose-dependent, but at doses used in this study (10 mg/kg b.i.d.), the first signs of motor impairment occur 4 to 6 days after dosing begins. Rats were fed with diet containing 1% creatine, or normal control diet, for two weeks before 3-NP administration. 3-NP (10 mg/kg i.p. b.i.d.,) or vehicle (PBS, Iml/kg i.p. b.i.d.) was administered for 3 days. On the morning of the fourth day (3 days post first injection), rats underwent the 2DG procedure (as described in the original procedure).

Animals: 44 males Sprague Dawley rats (250-300g at start) were used. Six rats were excluded after the creatine feeding period due to exceeding maximum weight limits for the 2-DG procedure (420g). Three more were excluded on the basis of weight after the 3-NP treatment period. Two rats died during the 3-NP administration period. 33 rats underwent the 2-DG procedure. Of these, ten were excluded from the final analysis on the basis of abnormal glucose or blood gas levels, or poor radionuclide perfusion.

Physiological Variables: Arterial plasma glucose, blood gases, blood pressure, and rectal temperature were recorded 5 minutes before beginning the 2-DG procedure ("Pre" values), and 35 minutes into the procedure (10 minutes before termination). Data are presented in Table 16. Glucose and temperature were measured throughout the procedure. Arterial plasma glucose levels, pO2 and pCO2 tensions, and blood pressure did not differ between creatine/control fed rats, or between 3-NP/vehicle treated rats. Arterial pH and body temperature showed small magnitude reductions in 3-NP rats that received creatine, versus rats fed control diets, but levels remained well within normal physiological ranges and should not impact glucose use rates. There were no

Table 16: Physiological Variables in 1% creatine or control treated rats, following 3-NP.

		Con/PBS	Con/3-NP	Cre / PBS	Cre / 3-NP
Glucose	Pre	156.0 ± 6.8	200.6 ± 23.1	160.3 ± 5.9	195.7 ± 27.2
Glucose	+ 35 min.	154.6 ± 7.6	209.0 ± 17.1	171.2 ± 6.9	188.6 ± 28.7
p_aO_2	Pre	82.7 ± 1.0	87.0 ± 2.0	88.3 ± 4.5	87.5 ± 3.3
p_aO_2	+ 35 min.	84.3 ± 1.9	94.6 ± 2.5 †	87.2 ± 3.5	92.8 ± 1.8
p_aCO_2	Pre	39.4 ± 1.1	39.8 ± 0.8	39.6 ± 1.0	38.1 ± 1.1
p_aCO_2	+ 35 min.	37.3 ± 0.6	35.7 ± 1.6	39.7 ± 1.2	35.3 ± 1.2
pH	Pre	7.5 ± 0.0	7.4 ± 0.0	7.5 ± 0.0	7.4 ± 0.0 **
pH	+ 35 min.	7.5 ± 0.0	7.4 ± 0.0	7.5 ± 0.0	7.4 ± 0.0 *
BP_a	Pre	132.3 ± 0.9	132.5 ± 2.1	133.0 ± 1.0	139.2 ± 4.9
Temp °C	Pre	37.0 ± 0.1	37.0 ± 0.0	37.1 ± 0.1	37.1 ± 0.1
Temp °C	+ 35 min.	37.1 ± 0.0	37.1 ± 0.1	37.2 ± 0.0	37.0 ± 0.1 *
Number of animals		7	7	6	7

Data are mean ± SEM for: arterial plasma glucose (mg/dL), blood gases and pH (mmHg), arterial blood preesure (BP_a, mmHg), and temperature (ßC). Levels measured immediately before isotope injection (Pre) and at the end of the 2-DG procedure (+35 min). Rats received creatine (Cre) or control (Con) diet, and 3-NP (10mg/kg i.p., b.i.d.) or vehicle (PBS, 1ml/kg i.p., b.i.d.). * $p<0.05$, significant difference relative to PBS/3-NP group (ANOVA, followed by Fisher s PLSD post-hoc unpaired t-test).

significant alterations in any parameters within animals over the duration of the procedure (Students' paired t-test, $p > 0.05$), indicating rats were not stressed during the experiment.

Glucose Use: Glucose use was measured in twenty brain regions, chosen to include multiple areas throughout the striatum (where 3-NP eventually induces cell loss); regions anatomically associated with the striatum, and control regions (cerebellum and white matter) (Table 17). We found no significant alterations in glucose use between 3-NP injected and vehicle-injected rats, or between creatine and control treated rats (with or without 3-NP). Values in control diet/vehicle rats were generally higher that in other groups, but differences did not reach statistical significance. Presence or absence of striatal lesions in these rats was examined using cresyl violet staining. None of the rats in this study showed striatal cell loss (data not shown).

Table 17: Local Cerebral Glucose Utilization ($lCMR_{glc}$) following 3-NP administration, in 1% creatine or control treated rats.

REGION	Norm/PBS	Norm/3-NP	Cre / PBS	Cre / 3-NP
Frontal Cortex I-III	102 ± 7	85 ± 10	87 ± 5	89 ± 11
Frontal Cortex IV	117 ± 7	102 ± 11	103 ± 5	108 ± 12
Frontal Cortex V-VI	87 ± 6	76 ± 8	77 ± 3	79 ± 9
Rostral Striatum: Dorsolateral	98 ± 8	88 ± 11	83 ± 4	88 ± 10
Ventromedial	88 ± 6	77 ± 10	78 ± 3	78 ± 11
Dorsomedial	84 ± 8	75 ± 11	74 ± 3	76 ± 10
Striatum: Dorsolateral	93 ± 5	84 ± 10	83 ± 5	82 ± 11
Dorsolateral Rim	99 ± 5	90 ± 12	86 ± 5	86 ± 9
Ventromedial	91 ± 7	77 ± 10	75 ± 3	74 ± 9
Dorsomedial	94 ± 8	80 ± 11	83 ± 6	78 ± 9
Caudal Striatum	91 ± 5	80 ± 11	74 ± 3	80 ± 9
Globus Pallidus	55 ± 4	49 ± 8	45 ± 2	49 ± 7
Hippocampus: CA1	61 ± 4	48 ± 8	48 ± 3	49 ± 6
CA3	77 ± 4	65 ± 9	61 ± 4	63 ± 7
Dentate Gyrus: Molecular Layer	84 ± 8	86 ± 10	75 ± 3	81 ± 10
Nucleus Accumbens	87 ± 7	76 ± 11	71 ± 4	75 ± 8
Substantia Nigra: *pars reticulata*	51 ± 7	57 ± 10	44 ± 2	49 ± 7
pars compacta	81 ± 8	88 ± 8	69 ± 3	80 ± 14
Cerebellum: Grey matter	60 ± 4	57 ± 7	52 ± 3	50 ± 6
White matter	29 ± 4	32 ± 4	27 ± 2	26 ± 4
Number of Animals	6	5	6	6

Data are mean ± SEM for: $lCMR_{glc}$ (nmol/100g/min). Rats received creatine (Cre) or control (Con) diet, and 3-NP (10mg/kg i.p., b.i.d.) or vehicle (PBS, 1ml/kg i.p., b.i.d.). $p > 0.05$ (ANOVA).

Discussion: Results suggest that no abnormal alterations in glucose use occur in the striatum of rats following 3 days of 3-NP administration, prior to cell degeneration in this region. In the

original proposal we intended to measure glucose use in this model at multiple time-points preceding lesion formation. However, on the basis of the current evidence of no metabolic changes after 3 days of 3-NP administration, we will not examine earlier time-points at this 3-NP dose. We have, however, conducted pilot studies to try to determine a useful time to detect any presymptomatic, pre-lesion glucose use changes (if any exist), in rats treated with 3-NP for longer periods. Preliminary studies indicate that rats showing the first signs of motor impairment exhibit marked reductions in glucose use in the striatum, but only in regions where cell loss is already evident (data not shown). To date, we have not been able to detect any significant alterations in glucose use prior to cell degeneration in the striatum.

The observations reported appear to be consistent with an "all or nothing" effect of 3-NP on glucose use, suggesting that perhaps a critical threshold of complex II inhibition needs to be reached before cell dysfunction and metabolic impairment occur, and after this point cells degenerate rapidly. This hypothesis is not proven by our data, however, since it is not possible to determine exactly when motor impairment and cell loss *would have* occurred in the animals used in the study. A major problem with 3-NP toxicity studies is that there is large inter-animal variability in the time to symptom onset after dosing. Rat strains also vary in vulnerability. Hence, it is difficult to predict when an animal is close to developing striatal defects. However, our data do suggest that if energetic changes *do* occur in this model before cell loss, they occur later that 3 days into the course of 3-NP treatment (with the dose and rat strain used in this study).

7. KEY RESEARCH ACCOMPLISHMENTS

1) The finding that cerebral glucose use is not significantly altered in *Hdh*^{Q50} CAG knock-in mice at 4 months of age, relative to levels in wild type animals; and that no gene dosage effect is seen in *Hdh*^{Q50} mice (48/48 vs. 48/7 CAG repeats).

2) The finding of impaired activities of complexes II-III and IV of the electron transport chain in *Hdh*^{Q50} and *Hdh* ^{Q92} mouse brain cerebellum at 4 months of age (preceding symptom onset and NII formation).

3) The finding that aconitase activity is increased in the cerebellum of *Hdh*^{Q50} (48/48) mice at 4 months of age.

4) The finding that cerebral glucose use is reduced in several forebrain regions in the G93A transgenic mouse model of FALS at 60 days of age – a time point preceding the onset of the first pathological changes in these mice.

5) The finding of increased complex I activity in the forebrain of G93A mice at 60 days of age, indicating impaired mitochondrial energy metabolism consistent with the defect seen in FALS A4V patients with a SOD1 mutation, which precedes onset of symptoms and pathological changes.

6) The finding that cerebral glucose use is significantly increased in *Hdh*^{Q92} CAG knock-in mice at 4 months of age, relative to levels in wild type animals, and relative to levels in *Hdh*^{Q50}mice (Year 1 results).

7) The finding that cerebral glucose use in *Hdh*^{Q92} CAG knock-in mice shows a gene-dosage effect, with homozygote (90/90 CAG repeat) mice showing increased glucose use elevations than heterozygote (90/7) mice. In fact, the magnitude of glucose use increases in 90/90 mice is approximately double levels in 90/7 mice.

8) The finding that alterations in cerebral glucose use in *Hdh*^{Q92} mice is evident at 4 months of age in these animals (the earliest time-point investigated). These changes precede pathological or behavioral changes in *Hdh*^{Q92} mice. (NB: *Hdh*^{Q92} mice do not develop a movement disorder, unlike *Hdh*^{111} mice and other HD transgenic mouse models). There is evidence that mutant huntingtin protein (*htt*) is translocating to the nucleus at this time-point, but neuronal intranuclear inclusions (NII) are not evident until 15 months of age in this model (Wheeler et al., 2000). Aggregate

formation occurs faster in *Hdh*^{Q111} mice, hence we are currently examining the same parameters of energy metabolism in these animals.

9) The finding that presymptomatic increases in glucose utilization also occur in multiple forebrain regions in another transgenic HD mouse line, N171-82Q mice expressing a mutant human HD fragment with an 82 polyglutamine repeat. Taken together, findings suggest that metabolic compromise may be an early event in the pathophysiology associated with the expression of mutant huntingtin protein. Glucose use elevations suggest that cells may be attempting to increase glycolytic ATP production, or increase substrate feed into mitochondrial energetic pathways to compensate for a metabolic stress or blockade. The exact mechanism has yet to be elucidated.

10) The finding that R6/2 transgenic HD mice develop a diabetic profile, with onset at 7-8 weeks of age (around the time of movement disorder symptom onset).

11) Observations that metabolic enzymes which show impaired activity in late-stage HD patients (reduced complex II-III and IV in post-mortem brain) do not show evidence of altered activities in pre-symptomatic R6/2 HD mouse brains (whole tissue homogenate preparations; 3.5 and 8 week-old mice). Some alterations are evident in late-stage (12 week-old) R6/2 mice. However, the nature of the metabolic enzyme activities we detected did not correlate with observations in symptomatic HD patients (Browne et al., 1997), or with previously reported alterations in homogenate samples from 12 week old R6/2 mice (Tabrizi et al., 2000). It is possible that use of whole brain homogenate preparations is masking any subtle region-specific changes occur, for example in the striatum of R6/2 mouse brains. Therefore we are currently repeating these assays in striatal preparations from these mice.

12) The finding of increased lactate production in symptomatic HD mice, suugesting abnormal energy metabolism at this stage of the disorder in R6/2 mice. This observation is consistent with increased lactate generation seen in symptomatic HD patients.

13) Findings of increases in oxidative damage markers (OH8dG, hydroxyl radical generation, F2 prostaglandins and hydroxynonenol) in symptomatic R6/2 and N171-82Q mouse models of HD.

14) Increases in markers of oxidative damage to protein (carbonyls), but not lipid (malondialdehyde), were found in the G93A mouse model of FALS. Protein carbonyl levels were elevated in symptomatic mice (110 days), but not at earlier timep-oints in this mouse line.

15)The finding of reduced ATP levels in R6/2 HD mouse forebrain, and to a lesser extent in cerebellum.

16)The observation that cerebral glucose utilization in striatum does not appear to be significantly altered prior to lesion formation induced by 3-NP administration, in rats.

8 REPORTABLE OUTCOMES

Gregorio J, DiMauro J-P P, Narr S, Fuller SW, Browne SE. Cerebral metabolism defects in HD: Glucose utilization abnormalities in multiple HD mouse models. *Soc. Neurosci. Abs.* (2002) 28: *In press*

Browne SE. Disruptions of cellular energy metabolism in HD: evidence for treatment effects? *Frontiers in Neurodegeneration – Huntington's disease.* (2002).

Browne SE, DiMauro J-P P, Narr S. Metabolic changes precede phenotypic changes in mutant mouse models of HD. *World Federation on Neurology Research Group on Huntington's Disease* (2001) S8.

Browne SE, Yang L, Fuller SW, Beal MF. Metabolic changes precede pathologic changes in the G93A mouse model of a familial amyotrophic lateral sclerosis. *Soc. Neurosci. Abs.* (2001) 27: 580.6.

J-P P DiMauro, S Narr, MF Beal, Browne SE. Cerebral energy metabolism in mutant mouse models of Huntington's disease. *Soc. Neurosci. Abs.* (2001) 27: 432.1.

Browne SE, Andreassen OA, Hughes DB, Ferrante RJ, Jenkins BG, Beal MF. Cerebral energetic defects in transgenic animal models of Huntington's disease. *World Federation on Neurology Research Group on Huntington's Disease.* (1999) 18: 46.

Browne SE, Beal MF. Huntington's disease. In: Funtional Neurobiology of Ageing. PR Hof, CV Mobbs, Eds. *Academic Press* (2000) 711-725

Browne SE, Wheeler V, White JK, Fuller SW, MacDonald, M, Beal MF. Dose-dependent alterations in local cerebral glucose use associated with the huntingtin mutation in *Hdh* CAG knock-in transgenic mice. *Soc. Neurosci. Abs.* (1999) 25: 218.11.

Browne SE, Licata SC, Beal MF. Energetic defects in a transgenic mouse model of familial ALS. *J. Neurochem.* (1999) S27B.

Four manuscripts are currently in preparation.

9. CONCLUSIONS

The overall goals of this proposal were to gain insight into the roles of defects in CNS energy metabolism and oxidative stress in mechanisms of neuronal death and dysfunction in neurodegenerative disorders. Outcomes may impact therapeutic strategies for treatment of both degenerative disorders and neurotoxin exposure. Previous studies in human and animal models have implicated the involvement of mis-metabolism and oxidative damage in the pathogenesis of several neurodegenerative diseases including Parkinson's disease (PD). This project concentrated largely on using *in vivo* techniques in whole animal models of degenerative disorders, to gain insight into disease mechanisms at all stages of pathogenesis. We focussed on transgenic mouse models of Huntington's disease (HD) and amyotrophic lateral sclerosis (ALS), since these best exhibit the progressive phenotypic and neuropathologic changes characteristic of their respective human disease profile. Experiments aimed to determine the relative contributions and sequential order of bioenergetic defects and oxidative damage to cell death processes in different mutant mouse models of HD and one transgenic mouse model of familial ALS (fALS). We also investigated in rats the CNS effects of a potent, systemically active mitochondrial toxin, 3-nitropropionic acid (3-NP), that induces cerebral lesions and behavioral changes closely resembling HD in several different species, including humans. We have been successful in completing the majority of studies outlined in our specific aims, and have initiated studies to augment findings from the original proposal.

Studies in the three years of this grant generated several novel observations of presymptomatic energetic abnormalities in both HD and ALS models. Firstly, we found that cerebral glucose utilization is markedly elevated in the forebrain of mice expressing the HD mutation. Most interestingly, this hypermetabolism occurs prior to any evidence of pathologic changes or symptoms in these animals. Further, we have recapitulated this observation in *two* distinctly different HD mutant mouse models: Hdh^{Q92} "knock-in" mice expressing a mutant expansion of the disease-causing CAG repeat in the murine homologue *HD* gene (expressing 90 CAGs that encode 92 glutamines, Q92) (White et al., 1997); and N171-82Q mice expressing a fragment of human huntingtin gene containing a mutant CAG repeat length (82 CAGs) (Schilling et al., 1999). Experiments in mice expressing different CAG repeat lengths suggest that this effect is CAG length-dependent, and shows a gene dosage effect. Another point of interest is that glucose use changes are not restricted to brain regions susceptible to degeneration, ie. the striatum.

This observation supports suggestions that striatal neurons are especially vulnerable to metabolic stress. Increases in glucose uptake prior to any pathologic changes suggest increased glucose demand to fulfill cells' functional requirements, perhaps due to impaired metabolic enzyme activity, uncoupling of mitochondria, and/or increased dependence on glycolysis. We have therefore commenced studies to examine the functional capacities of components of the glucose metabolic pathway in these HD mice, in search of potential sites of dysfunction. Initial studies suggest that ATP synthesis is sub-optimal in N171-82Q mice, but we found that activities of mitochondrial enzyme complexes II and IV (known to be defective in late stage HD) are normal in the forebrains of three different HD mouse lines, *Hdh*^{Q92}, N171-82Q, and R6/2. Findings would also be augmented by further documentation of the time-course of energetic changes as the phenotype develops in these mouse models. We have also found evidence of increased oxidative damage to DNA and lipids in a third transgenic mouse model of HD (R6/2 line), although preliminary results suggest the changes occur relatively late in the disease progression. In addition, elevated basal levels of hydroxyl radical production were observed in N171-82Q striatum.

In addition to mouse lines expressing the HD mutation, another approach to model the disease is to directly inhibit mitochondrial enzyme complex II. Impaired activity of this enzyme occurs in late stage HD (Browne et al., 1997), and experimental or environmental exposure to an agent that specifically inhibits this enzyme (3-NP) produces pathological lesions and phenotypic changes similar to HD (Ludolph et al., 1992). In studies in the rat, we found striatal neurons to be selectively vulnerable to 3-NP toxicity despite widespread complex II inhibition throughout the brain. However, in contrast to presymptomatic changes in genetic models, significant reductions in glucose use following 3-NP intoxication coincided with neuronal loss in this mouse line. Therapeutic approaches using pro-energy agents such as creatine have been shown (in other studies) to be neuroprotective in this lesion model (Andreassen et al., 2001). We believe this model provides a useful approach for further elucidation of regional vulnerability in HD.

In another mouse model of a neurodegenerative disorder, the G93A mouse model of familial ALS (overexpressing human mutant Cu/Zn superoxide dismutase, SOD-1), we also found a pattern of early metabolic changes that precede the first observations of neuronal pathology (mitochondrial disruption at ~70 days) and symptom onset (~100 days). Studies revealed reduced glucose utilization in brain and spinal cord at 60 days of age, concomitant with increased

mitochondrial complex I activity in these mice. Further, depletions in brain and spinal cord ATP levels were evident as early as 30 days of age. Elevated free radical generation is also evident in the cortex by 90 days (earliest time-point examined to date). In this fALS model, cells appear to have reduced capacity for glucose uptake before symptom onset, but the rate of complex I activity is elevated, perhaps in an attempt to increase electron transport and boost falling ATP production.

Results in mutant mouse models of both ALS and HD clearly demonstrate the early involvement of metabolic changes in the sequence of events initiated by expression of the mutant disease gene, prior to pathologic changes, symptom onset and cell death. The nature of the metabolic changes seen differs between the HD and ALS models, suggesting that the nature of triggering events set in motion by the gene defect may vary in these disorders. It still remains to elucidate the exact pathway from mutant gene expression to induction of metabolic changes. Overall, outcomes of these studies will have a great impact on the development of therapeutic strategies for these diseases and potentially for other neurodegenerative disorders in which metabolic dysfunction occurs, including PD and mitochondrial neurotoxin exposure. Results support the potential efficacy of pro-energy agents, or metabolism-enhancing agents, in therapeutic strategies for HD and ALS.

10 REFERENCES

Andreassen OA, Dedeoglu A, Ferrante RJ, Jenkins BG, Ferrante KL, Thomas M, Browne SE, Friedlich A, Hersch SM, Borchelt DR, Ross CA, Beal MF. Creatine increases survival and delays motor symptoms in a transgenic animal model of Huntington's disease. . *Neurobiol. Dis.* (2001) 8: 479-491.

Beal MF, Ferrante RJ, Browne SE, Matthews RT, Kowall NW, Brown Jr. RH. Increased 3-nitrotyrosine in both sporadic and familial amyotrophic lateral sclerosis. Ann. Neurol. 1997; 42:646-654.

Browne SE, Ayata C, Huang PL, Moskowitz MA, Beal MF. The cerebral metabolic consequences of nitric oxide synthase (NOS) deficiency: Glucose utilization in neuronal and endothelial NOS null mice. J. Cereb. Blood Flow Metab. 1999; 19:144-148.

Browne SE, Beal MF. Huntington's disease. In: Funtional Neurobiology of Ageing. PR Hof, CV Mobbs, Eds. *Academic Press* (2000) 711-725

Browne SE, Bowling AC, Baik MJ, Gurney M, Brown RH Jr, Beal MF. Metabolic dysfunction in familial, but not sporadic, amyotrophic lateral sclerosis. J Neurochem. 1998; 71:281-287.

Browne SE, Bowling AC, MacGarvey U, Baik MJ, Berger SC, Muqit MMK, Bird ED, Beal MF. Oxidative damage and metabolic dysfunction in Huntington's disease: selective vulnerability of the basal ganglia. *Ann. Neurol.* (1997) 41: 646-653.

Browne SE, Yang L, Fuller SW, Beal MF. Metabolic changes precede pathologic changes in the G93A mouse model of a familial amyotrophic lateral sclerosis. *Soc. Neurosci. Abs.* (2001) 27: 580.6.

Dal Canto, MC and Gurney, ME. (1995) Neuropathological changes in two lines of mice carrying a transgene for mutant human Cu, Zn SOD, and in mice overexpressing wild type SOD: a model of familial amyotrophic lateral sclerosis (FALS). Brain Res. 676: 25-40.

Ferrante RJ, Andreassen OA, Jenkins BG, Dedeoglu A, Kuemmerle S, Kubilus JK, Kaddurah-Daouk R, Hersch SM, Beal MF. (2000) Neuroprotective effects of creatine in a transgenic mouse model of Huntington's disease. J Neurosci 20:4389-97

Ferrante RJ, Browne SE, Shinobu LA, Bowling AC, Baik MJ, MacGarvey U, Kowall NW, Brown RH Jr, Beal MF. Evidence of increased oxidative damage in both sporadic and familial ALS. J Neurochem. 1997; 69:2064-2074.

Gu M, Gash MT, Mann VM, Javoy-Agid F, Cooper JM and Schapira AHV (1996) Mitochondrial defect in Huntington's disease caudate nucleus. Ann Neurol. 39: 385-389.

Guidetti P, Charles V, Chen EY, Reddy PH, Kordower JH, Whetsell WO Jr, Schwarcz R, Tagle DA. (2001) Early degenerative changes in transgenic mice expressing mutant huntingtin involve dendritic abnormalities but no impairment of mitochondrial energy production. Exp Neurol 169:340-50.

Gurney, M.E. *et al.* (1994) Motor neuron degeneration in mice expressing a human Cu, Zn superoxide dismutase mutation. Science 264: 1772-1775.

Menzies FM, Ince PG, Shaw PJ.(2002) Mitochondrial involvement in amyotrophic lateral sclerosis Neurochem Int 40:543-51.

Sokoloff, L, Reivich, M, Kennedy, C *et al.* (1977) The [^{14}C]2-deoxyglucose method for the measurement local cerebral glucose utilization. Theory, procedure, and normal values in the conscious and anaesthetized rat. J. Neurochem. 28: 897-916.

Tabrizi SJ, Cleeter MWJ, Xuereb J, Taanman JW, Cooper JW, Schapira AHV. (1999) Biochemical abnormalities and excitotoxicity in Huntington's disease brain. Ann. Neurol. 45: 25-32.

Tabrizi SJ, Workman J, Hart PE, Mangiarini L, Mahal A, Bates G, Cooper JM, Schapira AH. (2000) Mitochondrial dysfunction and free radical damage in the Huntington R6/2 transgenic mouse. Ann Neurol. 47: 80-6.

Wheeler VC, White JK, Gutekunst CA, Vrbanac V, Weaver M, Li XJ, Li SH, Yi H, Vonsattel JP, Gusella JF, Hersch S, Auerbach W, Joyner AL, MacDonald ME. (2000) Long glutamine tracts cause nuclear localization of a novel form of huntingtin in medium spiny striatal neurons in HdhQ92 and HdhQ111 knock-in mice. Hum Mol Genet. 9: 503-13.

Wheeler VC, Gutekunst CA, Vrbanac V, Lebel LA, Schilling G, Hersch S, Friedlander RM, Gusella JF, Vonsattel JP, Borchelt DR, MacDonald ME.(2002) Early phenotypes that presage late-onset neurodegenerative disease allow testing of modifiers in Hdh CAG knock-in mice. Hum Mol Genet. 11:633-40.

White JK, Auerbach W, Duyao MP, Vonsattel J-P, Gusella JF, Joyner AL and MacDonald ME. (1997) Huntingtin function is required for mouse brain development and is not impaired by the Huntington's disease CAG expansion mutation. Nature Gen. 17: 404-410.

11. APPENDICES

13. PERSONNEL

Personnel who received wages courtesy of this grant, were:

Dr. Susan E. Browne, PhD (PI)

Sara Fuller, BS

Jon-Paul DiMauro, BS

Jason Gregorio BS